To the Graduate Council:

I am submitting herewith a thesis written by Jeffrey E. Haymond entitled "Prediction of Liquid Water Content Distribution in an Altitude Test Cell Using the FASER Two-Phase Flow Code". I have examined the final copy of this thesis for form and content and recommend that it be accepted in partial fulfillment of the requirements for the degree of Master of Science, with a major in Mechanical Engineering.

Roy A. Crawford

R. A. Crawford, Major Professor

We have read this thesis
and recommend its acceptance:

Roy J. Schultz

A. D. Vatsi

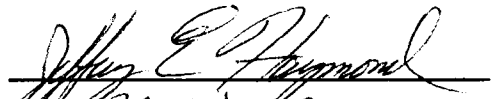
Accepted for the Council:

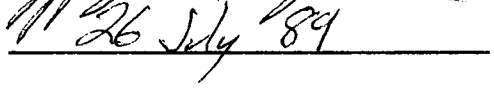
Vice Provost
and Dean of The Graduate School

STATEMENT OF PERMISSION TO USE

In presenting this thesis in partial fulfillment of the requirements for a Master's degree at The University of Tennessee, Knoxville, I agree that the Library shall make it available to borrowers under rules of the Library. Brief quotations from this thesis are allowable without special permission, provided that accurate acknowledgment of the source is made.

Permission for extensive quotation from or reproduction of this thesis may be granted by my major professor, or in his absence, by the Head of Interlibrary Services when, in the opinion of either, the proposed use of the material is for scholarly purposes. Any copying or use of the material in this thesis for financial gain shall not be allowed without my written permission.

Signature 

Date 

PREDICTION OF LIQUID WATER CONTENT DISTRIBUTION IN AN ALTITUDE TEST CELL USING THE FASER TWO-PHASE FLOW CODE

A Thesis

Presented for the

Master of Science

Degree

The University of Tennessee, Knoxville

Jeffrey Ethan Haymond

August 1989

ACKNOWLEDGMENTS

The research contained in this thesis would not have been possible without the generous use of the time and resources of the United States Air Force. In addition, without the help and inspiration of Dr. Dennis Lankford, Scott Bartlett and Gary Ledbetter, the effort would have been much harder and certainly more painful! And last but not least, I would like to thank my wife Jennifer for her patience and understanding in my times of frustration.

ABSTRACT

New aircraft/weapon systems are tested through a broad range of areas to insure safe and reliable use in actual flight operations. This testing traditionally is initiated in a ground test environment for safety and financial considerations. One area that must be examined prior to flight operations is the aircraft/weapon systems ability to perform its mission in icing conditions. The proper simulation of icing conditions in a test cell includes the requirement to have a uniform spatial distribution of Liquid Water Content (LWC).

The uniformity of the spatial LWC distribution is determined by the physical configuration of the test cell and the meteorological flight conditions being tested. A parametric study was performed to characterize the effects of changes to these parameters on spatial LWC for test cell J-1 in the Engine Test Facility. This characterization will be available to guide future efforts to improve the test cell design.

The two-dimensional two-phase flow code FASER was used to describe the effect of changes to test cell and meteorological parameters. This computer code provides qualitative plots to visually depict changes in spatial LWC uniformity. FASER was modified to include a calculation of the standard deviation and the mean of LWC. The standard deviation was used as a quantitative measure of the uniformity. A configuration from previous testing was used as a baseline condition. All changes made were compared to the baseline configuration. The results obtained are the first step in a FASER code calibration.

The results showed very little change for the meteorological parametric study. This indicates that similar uniformity is available throughout the range of icing conditions tested at the Arnold Engineering Development Center (AEDC). The test cell configuration parameters had a significant effect on uniformity. Careful test planning can take advantage of these results. The number of spray nozzles should be the highest possible to meet the total water flow required. The spray nozzles should be placed equidistant circumferentially but skewed outward radially. The area contraction ratio should be the highest possible. The bellmouth eccentricity should be as high as the area contraction ratio and bellmouth length will allow.

Future efforts must include acquisition of experimental data with known uncertainties to help in the code calibration. This data should be at the same conditions as performed in this parametric study. A subscale test program would provide the necessary data in a cost effective manner. The effect of varying more than one parameter at a time in the FASER program should be examined. Until the FASER code calibration is complete, the ability to accurately predict flight icing conditions in an altitude test cell will be limited.

TABLE OF CONTENTS

CHAPTER		PAGE
I.	INTRODUCTION	1
	A. Background B. Problem Statement C. Approach D. Baseline Condition	
II.	FASER COMPUTER PROGRAM	8
	A. Features and Equations B. Assumptions C. Graphical Output D. Modification E. Code Calibration Plan	
III.	METEOROLOGICAL TEST CONDITION PARAMETRIC STUDY	21
	A. Input B. Results C. Conclusions	
IV.	TEST CELL CONFIGURATION PARAMETRIC STUDY	27
	A. Input B. Results C. Conclusions	
V.	SUMMARY	36
	A. Conclusions B. Recommendations	
LIST OF REFERENCES		39
APPENDIXES		42
	A. Figures B. Tables C. Procedures for Changes to FASER Input	
NOMENCLATURE		87
VITA		89

LIST OF FIGURES

FIGURE		PAGE
1.	J-1 Icing Calibration System	44
2.	Baseline Nozzle Location	45
3.	Baseline Bellmouth (e = .93)	46
4.	J-1 Streamline Plot	47
5.	J-1 Trajectory Plot	48
6.	J-1 Topographical Plot of LWC	49
7.	J-1 Contour Plot of LWC	50
8.	J-1 Drop Distribution Plot 9.344 ft Downstream of Spraybars	51
9.	Grid Elements in J-1 Ducting	52
10.	Comparison of LWC Distributions Obtained for the Baseline Case and Case 2a with Increased Static Temperature	53
11.	Comparison of LWC Distributions Obtained for the Baseline Case and Case 4a with Decreasing Static Pressure at 3.217 ft	54
12.	Comparison of LWC Distributions Obtained for the Baseline Case and Case 4a with Decreasing Static Pressure at 12.25 ft	55
13.	Comparison of Drop Trajectory Plots for Cases 5a and 6a with Increasing Mach Number	56
14.	Comparison of LWC Distributions Obtained for Cases 9a and 10a While Varying Bulk LWC	57
15.	Bellmouth Curvature for Different Eccentricities	58
16.	Case 7b Nozzle Location (Inward)	59
17.	Case 4b Nozzle Location (Even)	60
18.	Case 6b Nozzle Location (Outward)	61
19.	Area Contraction Ratio Variation	62

20. AEDC 2050 Spray Nozzle 63

21. Comparison of Streamlines for Cases 1b and 2b Obtained While Increasing Eccentricity 64

22. Comparison of Drop Trajectory Plots for Cases 1b and 2b Obtained While Increasing Eccentricity..... 65

23. Case 3b Streamlines for Eccentricity of .97 66

24. Comparison of LWC Profiles for Cases 4b and 5b While Increasing the Number of Nozzles..... 67

25. Drop Distribution at 3.217 ft for Different Nozzle Locations ... 68

26. Drop Distribution at 12.25 ft for Different Nozzle Locations 69

27. Drop Distribution for Different Area Contraction Ratios 70

28. Drop Distribution for Different Bellmouth to Spraybar Lengths 71

29. LWC Profiles for Different Bellmouth to Spraybar Lengths 72

30. Drop Trajectory for Different Bellmouth to Spraybar Lengths 73

31. Baseline Ellipse..... 74

LIST OF TABLES

TABLE		PAGE
1.	Baseline Differences	76
2.	Meteorological Parameters and Code Input	77
3.	Meteorological Parametric Study Standard Deviation Comparison	78
4.	Test Cell Configuration Parametric Study	79

I. INTRODUCTION

BACKGROUND

During flight operations, aircraft and weapon systems can be exposed to icing conditions. The resulting ice accretion can decrease performance, cause engine damage and ultimately lead to the inability of the system to complete its mission. Therefore it is desirable to know the effects of exposure to icing conditions for each particular aircraft or weapon system and to design a protection system to avoid unacceptable system operation. Ice protection systems must be thoroughly tested in a ground test environment prior to flight operation for safety and financial considerations. It is critical that this ground test environment accurately reflects potential flight operation. Small variations in test cell parameters can significantly affect the anti-icing or de-icing capability of flight systems (Ref 1). Fortunately extensive work has been performed to map actual cloud characteristics (Ref 2).

Altitude test cells such as those at the Arnold Engineering Development Center's (AEDC) Engine Test Facility (ETF) have the capability to simulate an icing environment. Test cell J-1 typifies the icing test cells at AEDC (Ref 3). Exact duplication of all parameters that characterize icing conditions in flight is frequently not possible nor necessary to provide adequate simulation in an altitude test cell (Ref 4). Free-stream static or total conditions of temperature and pressure, Mach number, free-stream humidity, mean effective droplet diameter and Liquid Water Content (LWC) adequately define icing conditions (Ref 5).

Spatial LWC uniformity across the freejet exit of the tunnel has been defined as a necessity for acceptable icing testing. An uneven distribution could provide a more severe ground testing environment than nature would normally provide. To alleviate the problems of nonuniform LWC distribution, short duration ice accretion tests are made in the tunnel prior to test article installation. A steel mesh grid is installed at the bellmouth freejet exit to measure the ice accretion. The measured ice accretion is proportional to LWC. Figure 1* illustrates the ice accretion grid arrangement in test cell J-1. If the ice accretion is unacceptable, expensive trial-and-error testing is performed while making changes to the water spray nozzle installation to improve the distribution.

Many test cell configuration parameters can influence spatial LWC uniformity. These parameters include the area contraction ratio (area of the plenum/area of the freejet exit), bellmouth inlet curvature, nozzle position, and the number of spray nozzles. Other configuration parameters are dictated by the meteorological test conditions to be simulated such as droplet size distribution, static pressure and temperature, Mach number, and the bulk or total cell LWC.

It is important that a method be developed to characterize the effects of changes to the configuration parameters listed above. The characterization will assist in test cell preparation for icing tests with assured LWC uniformity. Currently, expensive test cell time with grid testing is used to provide optimization.

---

* All Figures are located in Appendix A and all Tables are located in Appendix B

A less expensive method of characterizing the effect of changes to the test cell configuration parameters above was developed in 1986. FASER, a two-phase two-dimensional flow code, was developed to model particle trajectories in a test cell environment (Ref 6). Test cell geometry and spray system design can be modeled with FASER and analyzed to determine their influence on downstream spatial LWC uniformity. While FASER has great potential for assisting in the preparation and set-up of icing tests in altitude test cells, this computer program has not been validated.

PROBLEM STATEMENT

Because FASER was not validated for use in icing test cell optimization, this research was defined in order to begin that validation process. Test cell J-1 is typical of test cells that FASER was designed to characterize and was selected for this study. The purpose of this thesis was to perform parametric studies of the effects of meteorological test condition and test cell configuration parameters on predicted spatial LWC uniformity for J-1 test cell of the Engine Test Facility (ETF) with the FASER computer code. The meteorological test condition parametric study examined the effects of changes to the static pressure and temperature, Mach number, mean effective droplet diameter, and total or bulk LWC. The test cell configuration parametric study examined the effects of changes to the number of spray nozzles, the area contraction ratio, the eccentricity of the bellmouth inlet curvature, the water injection velocity, the angle of spray injection, and the distance between the spraybars and the bellmouth entrance on spatial LWC uniformity. A validation plan for the code FASER was developed with incomplete areas identified.

APPROACH

The FASER computer code operation was examined listing the features and the governing equations. The assumptions made in the development and use of the code were listed and discussed. Minor modifications of the code were made to assist in the parametric studies. A validation plan for the FASER computer code was examined. The plan considered the requirements for a code calibration, those efforts that were done in this research, and those efforts that remain to be completed.

FASER was used to study the influence of changes to the meteorological and test cell configuration parameters listed previously for the ETF test cell J-1. For each parameter investigated, only that parameter was changed. A calculation was made with all other parameters held constant and equal to a specified set of parameters called the baseline condition. As previously discussed, the first parametric study examined the effects of changes to the meteorological test conditions. The meteorological test condition parameters were varied to each extreme in the icing envelope. Extremes of the icing envelope were obtained from FAA regulations (Ref 7). This parametric study was needed to understand the effects that different simulated flight conditions have on LWC uniformity. The second parametric study examined the effects of changes to the test cell design. The test cell configuration parameters were varied from the baseline condition to practical limitations of the current test cell design. The information obtained in this parametric study will assist in guiding future modifications to the test cell geometry to improve spatial LWC distribution. The graphical computer output was modified to include a calculation for the spatial LWC mean and

standard deviation. The mean and standard deviation calculations obtained for the baseline condition serve as a measure for comparison for all changes that result from the parametric studies.

BASELINE CONDITION

In 1982 the AEDC conducted an inlet icing test program in test cell J-1. Prior to initiation of this program, icing grid tests were performed to qualitatively assess LWC uniformity. The test cell configuration used during those grid tests was used as the baseline set of meteorological and geometrical parameters in this study.

The meteorological test conditions at the freejet exit were as follows:

Mach = .55

T_t = 480°R

Pressure Altitude = 1000 ft

MDD = 20 microns

LWC = .9 gm/m^3

The test cell geometric configuration parameters are as follows:

Number of Spray Nozzles = 10

Area Contraction Ratio = 4.76

Nozzle Location = (see figure 2)

Bellmouth Eccentricity = .93 (see figure 3 for curvature)

Water Injection Angle = 35 deg

Water Injection Velocity = 80 ft/sec

Distance Between Spraybars and Bellmouth = 5.329 ft

Spatial distributions of ice accretion thicknesses from the grid testing were available. However, the current method of comparison of spatial ice accretion to spatial LWC has some measurement uncertainty. Although heavier or thicker regions of ice accretion represent flow areas with greater LWC, a direct comparison was not performed. Eventually FASER should predict LWC distributions that correspond sufficiently well to measured ice accretion patterns or measured LWC distributions. However, this requires a validation process beyond the scope of the present study. This type of validation process will be discussed later in terms of the experimental data sets required. For the present study, the predicted LWC distribution obtained with FASER for the baseline condition serves only as a reference condition to which the changes obtained in the parametric studies can be compared.

There was one major difference between the baseline configuration above and the previous calibration configuration. The number of spray nozzles in the code parametric study was reduced from 75 that were actually used in the grid testing to 10 for simulation. This was done for two purposes. First, the amount of computer time was significantly reduced. Second, initial code development had shown spatial LWC to be mixing limited (Ref 6). This means that a spray does not tend to spread without an external forcing mechanism. An increase in the number of nozzles would provide an external mechanism for improved mixing in the test cell. With a large number of nozzles, the spatial distribution of LWC was relatively good. However, a parametric study requires that the results be clearly attributable to input

parameter changes. A large number of spray nozzles would not permit this to occur. That is, the effects of a large number of spray nozzles may overwhelm all other effects. Therefore, for the parametric studies of this research program, a set of 10 nozzles was used in order to clearly demonstrate the effects of the parameters studied. Note, however, that in the complete validation study ultimately required for FASER, the number of nozzles used experimentally and in testing must be identical.

II. FASER COMPUTER PROGRAM

FASER is a two-dimensional two-phase flow code designed to analyze spraying systems within a test cell. It was developed to minimize trial-and-error ice accretion grid testing to establish acceptable spatial liquid water content uniformity at the engine inlet station. FASER allows comparison of different configurations to be done quickly and inexpensively.

FEATURES AND EQUATIONS

FASER features two modules, POTFLOWX and TDROP. The POTFLOWX module controls ten subroutines which calculate a potential flowfield solution for compressible, inviscid, isentropic flow. Alternately, a two-dimensional flowfield may be read into the program. TDROP is the heart of the FASER program. This module controls all aspects of the droplet trajectory process with 32 subroutines. It includes turbulence as well as evaporation and condensation. For a detailed explanation of the FASER code operation, Ref 6 should be examined.

Some of the controlling equations used in FASER are presented here to illustrate the capabilities and the inherent limitations within this code. The rest of the equations incorporated in FASER are available in Reference 6.

To calculate the gas phase potential flow, the isentropic, compressible stream function equation (1) is solved using an alternating direction implicit method

$$\frac{\partial}{\partial y}\left(\frac{\rho_0}{\rho}\,\frac{1}{y^J}\,\frac{\partial \Psi}{\partial y}\right)+\frac{\partial}{\partial x}\left(\frac{\rho_0}{\rho}\,\frac{1}{y^J}\,\frac{\partial \Psi}{\partial x}\right)=0 \qquad (1)$$

where the stream function is defined by

$$u = \frac{\rho_o}{\rho} \frac{1}{y^J} \frac{\partial \psi}{\partial y} \qquad v = \frac{-\rho_o}{\rho} \frac{1}{y^J} \frac{\partial \psi}{\partial x} \tag{2}$$

where j = 0 planar flow

j = 1 axisymmetric

Equation (1) is a statement that the flow is irrotational. Assuming isentropic flow, the energy equation provides the final information necessary

$$\frac{\rho_o}{\rho} = \left[1 + \left(\frac{\gamma - 1}{2}\right) M^2\right]^{\frac{1}{\gamma - 1}} \tag{3}$$

Initial and boundary conditions are given as input to provide a two-dimensional gas phase flow field.

The most critical part of the computer program is the droplet trajectory model. The governing equation in the droplet trajectory model is the particle equation of motion

$$m_d \frac{d\overline{V}}{dt} = C_D \rho (\overline{U} - \overline{V}) | \overline{U} - \overline{V} | \frac{A_d}{2} + m_d \overline{g} \tag{4}$$

where the drag coefficient is given by Oseen's equation (Ref 6) as

$$C_D = \frac{24}{Re} + \frac{6}{1 + \sqrt{Re}} + .3 \tag{5}$$

The droplet Reynold's number is defined by

$$Re = \rho \frac{| \overline{U} - \overline{V} | d}{\mu} \tag{6}$$

FASER uses a K-ε turbulence transport model to simulate the turbulence that exists within a test cell. Spray turbulent intensity and a characteristic length scale are inputs needed to generate a fluctuating velocity term through the following equations:

$$\overline{u} = \overline{u} + \overline{u'} \tag{7}$$

where the mean velocity is described by a Gaussian probability distribution parameterized by the root-mean-square, or standard deviation, of the fluctuating velocity component, u'.

$$f(\bar{u}) = \frac{1}{\sigma\sqrt{2\pi}} \exp\left[-(\bar{u})^2 / 2\sigma^2\right] \tag{8}$$

The standard deviation is related to the turbulent kinetic energy level assumed as an input condition

$$\sigma = \left(\frac{2}{3} K\right)^{.5} \tag{9}$$

In order to establish time-scales for the integration of particle motion, FASER uses the time scales appropriate to turbulent fluctuations. It is assumed that the fluctuating velocity is held constant over a period of time. This period of time is the minimum of the eddy lifetime or the time required for a particle to cross an eddy

$$t = \min(t_e, t_t) \tag{10}$$

A turbulent dissipation length scale was determined by Shuen, et. al., (Ref 8) as

$$L_e = C\mu^{.75}K^{1.5}/\varepsilon \tag{11}$$

Eddy lifetime can then be calculated from

$$t_e = L_e/(2K/\varepsilon)^{.5} \tag{12}$$

and the eddy transit time can be calculated from

$$t_t = L_e / |\bar{U} - \bar{V}| \tag{13}$$

The turbulence inputs have been obtained empirically to match spray data from a single spray nozzle in AEDC research test cell R1D. R1D is an icing research cell with an 18 inch diameter duct featuring four spray nozzles. At the time this data was gathered, R1D was using a 12 inch diameter duct with a single spray nozzle. This approach assumes that some of the results from R1D can be translated to a multiple spray nozzle arrangement such as in test cell J-1; specifically, the characterization of the spray from the nozzle,

including the droplet size distribution, particle velocities, initial spray injection angles, etc.

ASSUMPTIONS

To calculate droplet trajectories, the FASER program makes several assumptions. A review is made below of the assumptions and their validity for an engineering approach to assist in test cell optimization. These assumptions are listed and discussed in the following paragraphs:

1. Gas-phase flow is two-dimensional axisymmetric and isentropic (particle-phase flow is three-dimensional).
2. The particle-phase is coupled to the gas phase, but the gas-phase flow is not affected by the particle-phase (one-way coupling)
3. All gases are ideal.
4. Water vapor is a trace specie in the gas phase.
5. The droplet size distribution of the spray can be characterized by groups of discrete droplet sizes.
6. Droplet interactions are neglected.
7. Droplets are spherical.
8. Droplet vaporization and condensation processes are diffusion limited.
9. A dominant flow direction can be defined.
10. Flow is subsonic if stream function solution is used.
11. Pressure force, apparent mass force, and Basset History integral ignored in trajectory equation.
12. Free convection effects ignored.

13. The streamline adjustment to the inlet design is constant and may be approximated by a smooth curve.

The first assumption is that the gas phase flow can be treated as two-dimensional, axisymmetric and irrotational. For test cell J-1 in the freejet mode, the assumption is valid. In the plenum area, especially around the spray bars, this assumption is invalid. However, due to the low velocities in this area ($M<.1$), this should not significantly affect conditions downstream. As the flow accelerates through the bellmouth, the streamlines are predominately axisymmetric. For an engineering model, a fully three-dimensional code would not be practical.

In typical icing conditions tested at AEDC, the droplet concentration is dilute. The mass flow of the air is generally two orders of magnitude larger than the mass flow of the water. This justifies assumption 2 that the droplet phase to gas phase is coupled one-way (Ref 9). For the conditions tested, air closely follows ideal gas behavior. Assumption 4 is necessary to fix the molecular weight in the equation of state calculation for a potential flow solution. Again this is acceptable for a dilute flow. Assumption 5 is simply an easy way to characterize the spray for bookkeeping purposes. Since in nature no two clouds are exactly alike, this assumption does not limit the code's ability to compare to a generic cloud. In a dilute flow, assumption 6 is acceptable except in the nozzle nearfield. Assumptions 2, 4, and 6 could be invalid in that area. To compensate, the nozzle nearfield was modeled empirically. Data from test cell R1D was matched with the code by varying the turbulence parameters and the water injection velocity (Ref 6). With the nearfield modeled empirically, assumption 6 is acceptable for the dilute particle loading that typifies an icing test.

A defined particle shape is necessary for the drag calculation as well as in the mass conservation equations. According to Sturgess, et. al. (Ref 10), a spherical shape is most likely for small particles (< 200 microns). A spherical particle entrained in a flow is likely to vaporize and condense at a much faster rate than it would diffuse. The icing conditions of interest will always be subsonic.

In calculating the particle equation of motion, the pressure force, apparent mass force and Basset history integral are ignored. Nichols (Ref 11) showed that these effects were small in relation to the drag and gravitation effects. Work by Faeth (Ref 9) supports this assumption.

The computer code input required a continuous, fixed outer test cell boundary to calculate the streamlines of the flow. The actual physical configuration of the test cell does not have this constant outer boundary. There is a possibility that pressure fluctuations between the edge of the bellmouth lip and the eight foot diameter plenum exist. The FASER code and this parametric study did not consider this possibility. There has been no investigation at AEDC to characterize these potential pressure fluctuations. It is generally felt that the velocities in this bellmouth region are so low that any pressure fluctuations would be negligible.

GRAPHICAL OUTPUT

The graphical output from the computer program FASER provided the only method of evaluation of different meteorological test parameters and test cell configurations. FASER integrates the particle information to provide continuum properties in a graphical format.

There are several different types of plots available with the computer program. The first plot available is of the streamlines from the potential flow solution. This plot covers the entire length of the duct (Figure 4). The remainder of the plots are generated with information from the particle trajectory portion of the code. One plot tracks individual droplets throughout the length of the duct (Figure 5). This plot indicates the extent to which the droplet particles follow streamlines. The remaining plots are available at any axial location. The axial locations are chosen through the code input.

Spatial LWC is illustrated by three-dimensional surface plots (Figure 6) in a topographic fashion. The sharpness of the peaks and valleys on the plot illustrate the uniformity of the distribution. Two-dimensional contour plots are also available (Figure 7). Droplet distribution plots (Figure 8) show how the droplets mix and spread from the individual sprays. All of these plots provided a useful means of qualitative assessment. However, none provided a means for quantifiable assessment. It was decided to add a parameter for quantifiable assessment of the change in the spatial LWC uniformity.

MODIFICATION

The parameter chosen for assessment was the standard deviation of the LWC. The LWC is determined for each grid element within any axial cross-sectional area. Figure 9 shows the shape of all grid elements for a given cross section of inlet ducting. The computer code calculates a mean and standard deviation of the LWC by using every grid element LWC value as the i'th component in the following equations. The mean and standard deviation calculation of any variable x is provided by Holman (Ref 12).

$$X_m = \frac{1}{n} \sum_{i=1}^{n} X_i \tag{14}$$

$$\sigma = \left(\frac{1}{n} \sum_{i=1}^{n} (X_i - X_m)^2 \right)^{.5} \tag{15}$$

The mean of the grid element LWC values should closely approximate the bulk or total LWC for the entire test cell. The standard deviation calculation provides a useful, quantifiable method of comparison for LWC uniformity. For a given mean value, a more uniform cloud will result in a smaller numerical value of standard deviation. With the addition of the standard deviation calculation, both quantitative and qualitative methods of comparison were available. The numerical results of these calculations were then displayed on the LWC surface plots.

Initial computer runs of the baseline condition were made to verify this change to the program. The results showed the mean value being almost 17% lower than the bulk value of the LWC. Evaporation was not used and therefore not a factor in the difference. This difference was considered excessive and the method of calculation was closely scrutinized. The outer elements of the grid (Figure 9) typically have less water than inner elements due to droplet inertia. They also have less cross-sectional area due to curvature of the inlet ducting. With less of the duct area represented by the outermost elements, the amount of influence these elements have on the LWC calculation should be reduced accordingly. The calculation above made no such differentiation. The method of calculation had to be modified for an area weighted mean and standard deviation. The equations are as follows:

$$X_m = \frac{1}{A_{tot}} \sum_{i=1}^{n} X_i \, A_i \tag{16}$$

$$\sigma = \left(\frac{1}{A_{tot}} \sum_{i=1}^{n} (X_i - X_m)^2 \, A_i \right)^{.5} \tag{17}$$

With these equations in place, the baseline condition was rerun to evaluate the change in the value of the LWC mean. The percentage difference between the mean and the bulk LWC was reduced to slightly over 3%. This difference was considered acceptable; especially since the value of the mean is not a prime consideration. The relative change in the standard deviation of the LWC between computer test conditions is the most critical consideration since it is indicative of cloud uniformity. With the changes to the equations for the LWC mean and standard deviation in place, the meteorological parametric study was ready to be performed.

The results of the standard deviation calculations do have some inherent uncertainty. It was found during the comparison of the results of the meteorological parametric study (Chapter III) that the standard deviations calculated could vary for identical test cases. When making initial comparisons, some results did not seem to match the overall trends that were seen. The baseline condition, despite being within the bounds of the two cases evaluating pressure change, had a standard deviation a few percent outside the range of standard deviations calculated for pressure extremes. To examine how this could occur, ten identical cases of the baseline condition were run. The results of the ten repeated runs are shown in Table 1. Due primarily to the stochastic nature of the turbulence in the code, there was up to 6% difference in standard deviations for identical cases. This difference

was more than enough to explain the baseline standard deviation being outside the standard deviation band for the pressure extremes. The difference in standard deviations suggests that parameters that are only changed a few percent in the parametric studies have an influence that cannot be identified due to the calculation uncertainty. The first baseline condition tested in fact had the lowest standard deviation of all baseline runs made. The mean of all the baseline LWC means was taken to use for comparison in the parametric studies while the individual runs were not repeated. Although trends were observed, due to the calculation uncertainty conclusions were not drawn when only small changes in standard deviation were present.

CODE CALIBRATION PLAN

The FASER computer program has not been validated. The capability to validate this code is currently unavailable because of the limited amount and the uncertainty of the experimental data. Validation implies that all features of a code are correctly modeled (Ref 13) within specified ranges of parameters. A Computational Fluid Dynamics (CFD) calibration measures a code's capability to predict specific parameters without verifying that all of the features are correctly modeled. This seems like a more viable option.

There are three distinct functional areas that must be assessed or calibrated. The first is the code's ability to accurately predict trends observed when changes are made to code input. If one parameter is systematically and monotonically varied, does the code accurately predict whether the LWC distributions become more or less uniform? The second area concerns the code's sensitivity to variations of specific parameters. For example, if the

code predicts that the area contraction ratio has more influence on spatial LWC distribution than the number of spray nozzles, does the empirical evidence confirm this? The first two functional areas concern the code's ability to predict relative changes in spatial LWC. The third area concerns the code's ability to predict absolute levels of LWC. How accurate can the code predict absolute levels of LWC and LWC statistical deviations? These are questions that must be answered for a complete FASER code calibration.

Work has been initiated to answer all three of these questions. In the present study, the code has been used (see Chapters III and IV) to characterize the effects of varying individual parameters. Where possible, the results were compared to the governing equations and physics. The code was also used to characterize the relative influence of individual parameters on spatial LWC uniformity (see Chapters III, IV, and V).

The code's ability to predict absolute LWC levels was briefly examined in Ref 6. Experimental LWC and mass flux data from test cell R1D using a single spray nozzle was compared to the FASER computer data. Comparison of the LWC data shows reasonable agreement of the shape and dispersion of the spray. However the values of the mass flux data from the FASER program are roughly ten times that of the experimental data. The experimental data is suspect due to the data acquisition method. The Optical Array Probe (Ref 6) used in R1D may not measure all droplets in the field of measurement. One droplet may occlude observation of other droplets. Also if there is any error in the measurement of the droplet diameter, this error will be cubed in the mass flux calculation. The measured mass flux did not correspond to the known level of water injected into the test cell. However

this does not explain a difference of this magnitude. Clearly more code development is necessary for absolute LWC predictions.

The effort reported in this thesis is a starting point for a FASER code calibration. But much more work needs to be done. The parametric studies performed with FASER varied the parameters of interest to practical limitations for the test cell configuration items and to the extremes of the icing envelope for the meteorological parameters. To calibrate the code, experimental data with well defined uncertainties must be taken for the same conditions as used in the parametric studies of this thesis. This range of conditions would cover the likely areas of testing at the AEDC.

The biggest problem in any code calibration/validation is the lack of a practical method of measuring spatial LWC with low uncertainties. The current nonintrusive measurement systems available measure particle sizes in a given area. Particles which cross the area at the edge or cover the entire area are rejected. This causes the measured LWC to be too low. Experimental data with low uncertainties must be acquired before the FASER code can be calibrated for its ability to predict absolute LWC levels for a given configuration.

The current measuring capability may not prevent the calibration of FASER for relative changes measured in trend or sensitivity studies. If the measurement system is consistent albeit inaccurate, then trends developed by varying individual parameters and the relative influence between parameters can be verified experimentally. The current method to prepare a test cell for an icing test and verify spatial LWC uniformity is to install a grid at the end of the tunnel and measure ice accretion on the grid. As long as the other variables which affect ice accretion (i.e. droplet size) are not changed as

individual parameters are varied, the relative change in ice accretion should indicate a relative change in LWC. This could be used to calibrate the FASER code for relative changes.

III. METEOROLOGICAL TEST CONDITION PARAMETRIC STUDY

A parametric study was performed to examine the effects of changes to the meteorological test parameters on spatial LWC uniformity. The meteorological test parameters included static pressure, static temperature, Mach number, mean effective droplet diameter, and the bulk or total LWC in the test cell. The FASER code input file was modified to change these parameters from the baseline condition. Appendix C describes the procedures and methodology used to change the input to the code. This parametric study was performed to give a more complete understanding of how changes to the flight condition effect spatial LWC uniformity for a given test cell design. A parametric study of the effect of changes to the meteorological test parameters on the thermodynamic state at the compressor face of a turbine engine was performed by Willbanks and Schulz (Ref 5). However they did not examine the effects of those parameter changes on LWC or cloud uniformity.

INPUT

The meteorological test parameters listed above were varied to the extremes of the icing envelope as described in the FAA regulations (Ref 7) and summarized in Table 2. The range of parameters run in the parametric study is consistent with the typical range of conditions simulated during icing testing at AEDC. This range is representative of different icing conditions seen in actual flight operations. At static temperatures above 492°R, freezing conditions are not normally seen. At static temperatures below approximately 438°R, there is typically not enough moisture in the air to have

icing problems. Icing conditions are not typically found at altitudes above 20,000 ft. At Mach numbers greater than .8, the aerodynamic heating is sufficient to prevent icing problems. Cloud research (Ref 2) has shown the range of droplet sizes and LWC's chosen for this study to be representative of actual values.

RESULTS

The standard deviations of LWC for the individual test cases were compared to the baseline condition and the results are tabulated in Table 3.

Static Temperature Change

Cases 1a and 2a examined the effects of static temperature changes. Total temperature was allowed to vary to maintain the Mach number of the baseline condition according to the adiabatic relationship

$$T_T = T_S \left[1 + \left(\frac{\gamma - 1}{2}\right) M^2\right] \qquad (18)$$

Results of temperature variation showed little change in standard deviation from the baseline condition. As temperature warmed, the uniformity decreased. This trend agrees with governing equations. For an ideal gas, increasing temperature must result in decreasing density at constant pressure.

$$\rho = \frac{P}{RT} \qquad (19)$$

With decreased density, the drag component in the particle equation of motion (equation 4) is decreased. Plots which result from the Case 1a calculations were very similar to the baseline condition plots. There was no discernible difference between the plots of the two cases. Plots resulting from the Case 2a calculations begin to show slight differences from the

baseline. The topographical LWC surface plot of Case 2a (Figure 10) shows slightly larger differences between the peaks and valleys which correspond to the higher standard deviation.

Static Pressure Change

Cases 3a and 4a evaluate the change in spatial LWC uniformity due to pressure altitude variation. Static and total properties are varied according to the isentropic relationship to maintain constant Mach number.

$$P_T = P_S \left[1 + \left(\frac{\gamma - 1}{2}\right) M^2\right]^{\frac{\gamma}{\gamma - 1}} \qquad (20)$$

The standard deviation shows an upward trend for increasing altitude. As the altitude increases, density of the air decreases (holding temperature constant). The density decrease reduces the drag force in the particle equation of motion. The drag force is the dominant means of inducing mixing of the two-phase flow. With a drag force reduction, the particles tend to flow more with the streamlines.

A closer look at the plots of Case 4a shows that the decreased uniformity due to increased altitude is not the case in the nearfield of the spray nozzles. Figure 11 compares the spatial LWC uniformity 3.217 ft downstream of the spraybars. The standard deviation of the LWC is actually lower than the baseline condition despite a decrease in density. In the spray nozzle exit region, there can be large differences between the gas and particle velocities. In this region the velocity difference is the driving factor in the drag term of the particle equation of motion. As the particle approaches the gas velocity, the decrease in density becomes a more dominant factor. By the end of the bellmouth (12.25 ft downstream of the spray nozzles) where

the velocity difference is relatively small, the decrease in density of Case 4a has resulted in a higher standard deviation than the baseline (Figure 12).

Mach Number Change

Cases 5a and 6a examined the effects of Mach number variation. Static properties were maintained at the baseline values. Total properties were then adjusted with isentropic relationships to set the proper Mach number. Mach number variation gave almost no change in standard deviation indicating little effect on spatial LWC uniformity. Higher Mach numbers result in higher turbulent intensities. This should help to provide increased mixing. However with higher Mach numbers, it takes less time for a particle to cross turbulent eddies. This reduces the mixing effect of the higher turbulent intensities. The higher Mach conditions also require a higher static temperature in the inlet to achieve the same static temperature at the exit. From the discussion of Cases 1a and 2a above it was seen that higher static temperatures resulted in reduced spatial LWC distribution. The cumulative effects caused by the increased Mach number yield no difference in spatial LWC uniformity. The increased turbulent intensities do cause more erratic particle behavior in the inlet region as seen in a comparison of the droplet trajectories (Figure 13) of Cases 5a (Mach = .2) and 6a (Mach = .8).

Mean Effective Droplet Diameter Change

Changing the value of the mean effective droplet diameter (MDD) for Cases 7a and 8a which cover an expected icing range of $15 < MDD < 25$ did not significantly change the spatial LWC uniformity. There was only a 5% change in the LWC standard deviation for the MDD range checked. The parametric study does reveal a trend of decreasing uniformity for increasing

MDD. The effect of the increase in particle diameter is cubed in the droplet mass equation

$$m_d = \frac{\rho_d \pi d^3}{6} \qquad (20)$$

The resultant increase in mass gives the particle greater inertia. This reduces the ability of turbulence to mix the droplets. The increase in inertia also reduces the ability of the flow to keep the droplets entrained in the streamlines as the flow travels through the curvature of the bellmouth. This forces more particles towards the center of the duct.

Bulk LWC Change

The last parameter to be varied in the meteorological parametric study was the bulk LWC. LWC's normally seen in icing testing cover the range of $.3 < LWC < 2.0$. Changing the bulk LWC caused the largest changes in standard deviation. This does not indicate a large change in cloud spatial uniformity. The standard deviations should be considered relative to the mean. Comparison of standard deviations alone for the other cases in this study is possible since the mean is constant for those cases. As a percentage of the mean, the standard deviations of Cases 9a and 10a are within one-half of one percent. Graphically this is seen by examining the LWC surface plots (Figure 14). The magnitude of the spikes are vastly different but the general shape of the LWC plots are similar.

CONCLUSIONS

The meteorological parametric study varied selected parameters throughout the possible icing regions tested at the AEDC. For these

conditions, the parametric study did not show any great variation in spatial LWC uniformity. The largest range of standard deviations was seen when static pressure was varied, and it only changed by approximately 7%. Based on the 6% range of standard deviations seen for the ten baseline calculations, the actual variation could be slightly more or less. Over the range of possible test conditions, the order of relative importance to cloud uniformity is as follows: pressure, temperature, mean effective droplet diameter, bulk LWC, and Mach number. In general, the changes seen by the variation in the meteorological parameters could be explained by basic controlling equations and physics. This gives credibility to the code's results. The interpretation of these results gives a vital understanding of the meteorological parameters impact, but the small changes seen do not cause great concern about the AEDC's capability to provide similar cloud uniformity over a broad range of flight conditions.

IV. TEST CELL CONFIGURATION PARAMETRIC STUDY

A parametric study was performed to examine the effects of changes to the test cell configuration parameters on spatial LWC uniformity. The test cell configuration parameters included the bellmouth curvature, defined by the eccentricity of the elliptical bellmouth entrance, the number of spray nozzles, the location of the spray nozzles, the area contraction ratio (area of the inlet/area of the exit), water spray injection angle, water spray injection velocity, and the distance between the spray nozzles and the bellmouth. Appendix C and Reference 6 give a detailed explanation of how test cell configuration parameters are changed in FASER.

The purpose of this parametric study was to identify the most influential test cell configuration parameters on spatial LWC uniformity. This information will be available to guide future improvements to the test cell design.

INPUT

The test cell configuration parameters listed above were varied to the practical limitations of the current test cell design. The spraybar design, for example, was kept with a maximum of 96 spray nozzles at their current locations. The inlet diameter was maintained at eight feet. However some changes to the test cell had to be made in order to gain the desired information. The exit area was varied as was the bellmouth design. The first consideration was to obtain the necessary information. The second consideration was to minimize changes to the current test cell design to make changes as feasible as possible to implement.

The eccentricity of an ellipse describes the curvature of many bellmouths used in test cells (Ref 15). It provides a convenient parameter to quantify changes to the bellmouth curvature. The bellmouth configuration presently used in test cell J-1 has an eccentricity of .93. Figure 15 illustrates the curvature of the bellmouth with different eccentricities. A more severe curvature with e = .9 (Case 1b) and a less severe curvature with e = .96 (Case 2b) were run to determine their effects. The largest bellmouth possible with the current area contraction ratio and bellmouth length (e = .97) was also tested in Case 3b. Details of how the numerical values were chosen are included in Appendix C.

Ten spray nozzles were used as the baseline condition and represented a minimum number of nozzles used during the study. 32 nozzles were used in Case 4b as a mid-range configuration. The high number of nozzles was chosen as 75 in Case 5b to duplicate a previously used nozzle configuration. The results of calculations using the stated range of spray nozzles should adequately describe the effect of increased number of spray nozzles on spatial LWC uniformity.

The effect of nozzle location was examined as well. 32 nozzles were chosen for this portion of the parametric study. Case 7b included all nozzles contained within a 44 inch diameter circle (see figure 16) of the freejet exit area. This would indicate the extent to which droplets detrain from streamlines. If droplets do not follow streamlines, this configuration should provide the most particles in the outer portion of the duct. Configurations with 32 nozzles evenly dispersed (Figure 17) and with 32 nozzles located at the outermost portion of the spraybars (Figure 18) were also run in Cases 4b and 6b respectively.

The area contraction ratio (ACR), which is defined as the area of the inlet/area of the exit, was changed by reducing the exit area while maintaining a constant inlet area. The baseline configuration had an ACR = 4.76. The diameter of the exit was reduced by one foot resulting in ACR = 9.045 for Case 8b. Case 9b increased the ACR to 23.06 by decreasing the exit diameter by two feet from the baseline. The changes in ACR were chosen for ease of computer input. The three ACR's chosen (Figure 19) cover a range of normal applications for test cell J-1.

The baseline condition featured a water injection angle of 35 deg. The water injection angle is the angle between the spray centerline and the axial velocity component. This angle is built into the spray nozzles currently used at AEDC (Figure 20). To check for potential improvement in the mixing capability of spray nozzles, the spray angle was increased to 60 deg in Case 10b and 75 deg in Case 11b. The baseline water injection velocity was 80 ft/sec for the computer input. The actual water injection velocity is unknown. Since this factor is unknown and the value plays a critical role in the particle equation of motion, the effect of changing this parameter was examined. Since the particle equation of motion is really concerned with the difference in gas and particle velocities, the water injection velocity was increased for both cases. Case 12b raised the injection velocity to 160 ft/sec and Case 13b raised the injection velocity to 250 ft/sec. This eliminates the possibility that if, for example, the gas velocity is 60 ft/sec and a run was made with the water injection velocity = 40 ft/sec, that the information obtained would be the same as the baseline condition. Both cases would have a change in velocity = 20 ft/sec. Since in all cases tested the gas inlet velocity was less than 80 ft/sec, this could not happen in the parametric study.

The last parameter varied was the distance between the spraybars and the bellmouth inlet. The baseline distance was 5.329 ft. This distance was increased by one foot for Case 14b and was reduced by one foot for Case 15b. These distances were chosen for ease of code input and practicality of possible implementation.

RESULTS

The 15 cases examined in the test cell configuration parametric study were compared to the baseline configuration. The calculated standard deviations of the mean of LWC were compared and the differences from the baseline average are listed in Table 4. Some of the results did not agree with expectations. The parameters were each varied individually in an effort to characterize that parameter's influence. However, it will be seen that some of the computer runs inadvertently varied more than one parameter at a time. This caused some of the inconsistencies in the computer data.

Bellmouth Eccentricity Changes

Cases 1b, 2b, and 3b examined the effect of changing the bellmouth eccentricity. Case 1b increased the severity of the bellmouth curvature. Due to droplet inertia, it was expected that a more severe curvature would result in more droplets detraining from the streamlines and converging towards the center of the duct, giving a less uniform distribution. The computer results of Case 1b agreed with this expectation. The standard deviation was 1% higher for Case 1b over the baseline which represents a slightly less uniform distribution; albeit negligible with the computer calculation uncertainty.

The Case 2b configuration had an eccentricity of .96. This more gentle curvature was expected to force less droplets to the center of the duct and result in a more uniform distribution. The standard deviation of Case 2b, however, was 34% higher than the baseline! In an effort to reduce the bellmouth curvature, the Case 2b input had also reduced the distance between the spraybars and the bellmouth inlet by almost one foot. It will be shown in the discussion of Cases 14b and 15b that reducing this distance degrades the spatial LWC distribution. Referring to the streamline plots of Cases 1b and 2b (Figure 21), it is seen that the more gentle curvature of Case 2b forces the streamlines to adjust to the bellmouth sooner. In a comparison of the droplet trajectory plots of Cases 1b and 2b (Figure 22), it is seen that droplets exiting the spray nozzle in Case 2b do not mix upwards as in Case 1b due to the change in streamlines.

Case 3b was run to confirm that a more gentle bellmouth curvature with a sufficiently long mixing region would in fact result in an improved spatial LWC distribution. The streamline plot of Case 3b, featuring a bellmouth with eccentricity of .97, is shown in Figure 23. The standard deviation of this configuration did improve by almost 15% over the baseline condition.

Spray Nozzle Number Change

Cases 4b and 5b examined the effect of changing the number of spray nozzles. Reference 6 had concluded that the LWC distribution was mixing limited. Since increasing the number of spray nozzles would alleviate this problem, the spatial LWC distribution was expected to improve. Case 4b showed over 18% reduction in LWC standard deviation with an increase from

10 to 32 nozzles. Case 5b did not show as much improvement despite increasing to 75 nozzles. This may be due to the location of the 75 nozzles. The 75 nozzles were located as close to the center of the duct as possible. The spatial LWC distribution was in fact much more uniform in the center portion of the duct for Case 5b than for Case 4b. This is illustrated in a comparison of the LWC profile plots (Figure 24).

Spray Nozzle Location Change

Cases 4b, 6b, and 7b examine the effect of changing spray nozzle location. The spray nozzle radial location proved to be a very important parameter for LWC distribution. With the 32 spray nozzles located more outward radially on the spraybar system (Figure 18), Case 6b had a LWC standard deviation almost 43% lower than Case 7b which had nozzles located in the center of the duct (Figure 16). Case 7b actually had a 32% higher standard deviation than the baseline. The droplet distribution plots graphically illustrate the difference in location. Figure 25 compares these plots at X = 3.217 ft downstream of the spraybars. Case 6b starts out with a more uniform distribution. By the end of the duct, at X = 12.25 ft (Figure 26), the lack of mixing is evident. The majority of the droplets do follow streamlines and there is little water at the outer portion of the duct for Case 7b. Case 6b has more water droplets at the outer portion of the duct. However there is a lack of water observed at the center of the duct for Case 6b. The fact that droplets detrain from the streamlines and converge to the center of the duct during the passage through the bellmouth can be taken advantage of by choosing the spray nozzle location wisely.

Area Contraction Ratio Change

The largest improvement in LWC uniformity came by increasing the area contraction ratio. Case 9b reduced the standard deviation by over 37%. Convergence of the streamlines to a smaller exit area increases the number of droplets in the outer portion of the duct. A comparison of the baseline and Case 9b droplet distribution plots (Figure 27) illustrates this characteristic. The ability to take advantage of this improvement is dependent upon the size of the test article.

Water Injection Angle Change

The effect of changing water injection angle was examined in Cases 10b and 11b. Increasing the injection angle had a very small positive effect on the standard deviation. Considering the 6% variation seen earlier for different computer runs of the baseline condition, this effect is probably negligible. The visual evidence from the graphical plots also fail to show any significant differences.

Water Injection Velocity Change

The effect of changing the water injection velocity was examined in Cases 12b and 13b. The effect of these changes was again small. Increasing the relative velocity between the gas and the particle did increase the mixing and reduce the standard deviation (by up to 5% for Case 13b). Since the effect of large changes to the injection velocity is small, the fact that this velocity is currently unknown should not significantly restrict the use of this code.

Distance From Bellmouth To Spraybar Change

The distance between the spraybars and the bellmouth was the last parameter varied. Increasing this distance by one foot resulted in a 2.5% increase in standard deviation. The increase in distance allows the gravity term in the particle equation of motion (4) to have a more significant impact. Figure 28 illustrates this by comparing the droplet distribution plot of Case 14b to the baseline condition at X = 4.596 ft downstream of the spraybars. The large clusters of water particles are shifted down slightly for Case 14b. This results in heavier distribution at the bottom by the end of the duct. This is seen by comparison of the vertical LWC profiles (Figure 29). The vertical LWC spike on the bottom portion of the duct is 35% higher for Case 14b than the baseline.

Decreasing the distance between the spraybars and the bellmouth by one foot had a more significant impact. The standard deviation was increased by over 11%. The spray for Case 15b is not allowed to develop to its full potential. As discussed in Case 2b, the reduction in this distance forces the streamlines to adjust to the bellmouth much sooner, limiting the axial space available for the spray to mix. This may be due in part to the imaginary fixed outer boundary upstream of the bellmouth lip used in the FASER code. This effect is seen in a comparison of the droplet trajectory plots of Case 15b and the baseline (Figure 30). In the region from two to five feet, the Case 15b spray does not mix as much. This causes the degradation in spatial LWC distribution at the end of the duct.

CONCLUSIONS

Variation of the test cell configuration parameters can provide significant change in spatial LWC uniformity. Significant improvement in uniformity over the baseline condition is possible with careful consideration of the test cell design. The most influential test cell configuration parameter was the radial location of the spray nozzles with almost 43% variation between extremes. This is followed in order of importance by the area contraction ratio, the number of spray nozzles, the eccentricity of the bellmouth, and the distance between the spraybars and the bellmouth. The water injection angle and the injection velocity had virtually no effect on the cloud distribution. The order of influence is only true for the range of variation used in this study. In some cases, the range was picked arbitrarily for ease of code input.

However, the results shown above do give useful direction in planning an icing test to optimize spatial LWC uniformity. The easiest direction is to use the maximum number of nozzles possible for the amount of water flow planned. These nozzles should be spread equidistant circumferentially but skewed more to the outward radial locations. The area contraction ratio should be the largest that a test budget can afford. The test article size will determine the freejet exit area. The inlet area is determined by the size of the test cell with larger test cells being generally more expensive to operate. The eccentricity of the bellmouth should be increased as high as possible for the selected ACR and bellmouth length. The distance between the spraybars and the bellmouth should closely equal the baseline length for test cell J-1. Other test cells may need to scale this distance.

V. SUMMARY

A parametric study was made of the effects of meteorological and test cell configuration parameters on predicted spatial LWC uniformity in an icing test cell using a two-phase flow code called FASER. FASER was used to study these effects in a test cell geometry similar to the J-1 cell in the AEDC's Engine Test Facility. The requirements for a code calibration were examined. Current calibration progress was defined and remaining requirements were identified.

CONCLUSIONS

The FASER code needs to be calibrated for use as an engineering tool for application to icing testing. The calibration should be based on sets of experimental data with known uncertainties. The experimental data should be used to develop FASER to the point where it can predict trends as one variable is changed, predict the relative influence of different variables and predict the absolute levels of LWC at the engine inlet station of a test cell.

The present study attempted the first steps in the validation process for FASER by performing the meteorological parametric study which examined the effects of changes to pressure, temperature, Mach number, mean effective droplet diameter, and the bulk or total LWC on LWC distributions at the engine inlet station. These factors were found to have little influence on the spatial LWC uniformity. There should be no serious differences in uniformity for the flight conditions normally tested for icing. The trends observed did agree with governing equations giving some confidence in the code calculations.

The test cell configuration parametric study reported here examined the effects of changes to the bellmouth eccentricity, the number of spray nozzles, the location of the spray nozzles, the area contraction ratio, the water injection angle, the water injection velocity, and the distance between the spraybars and the bellmouth on the LWC distributions at the engine inlet station. These parameters had significant effects on spatial LWC uniformity as they were varied. The location of the spray nozzles was the most influential followed by the area contraction ratio, the number of spray nozzles, the bellmouth eccentricity and the distance between the spraybars and the bellmouth. Changes to the water injection angle and velocity had little impact. The order of the relative influence is only valid for the range of parameter variation used in this study.

RECOMMENDATIONS

The results of the study performed with FASER show that careful planning can help to optimize the test cell for spatial LWC uniformity. The number of spray nozzles should be the highest possible to meet the total water flow requirements. They should be placed equidistant circumferentially but with more placed outward radially. The area contraction ratio should be the highest possible. The bellmouth eccentricity should be as high as possible for a given area contraction ratio and bellmouth length. The distance between the bellmouth and the spraybars should be close to the baseline condition of 5.3 ft for the J-1 test cell.

Several other factors need to be further addressed. The uncertainty in the computer results discussed in Chapter II needs to be investigated and defined. The parametric studies performed in this study varied only one

parameter at a time. The impact of changing multiple variables needs to be studied. As mentioned previously, experimental data with known uncertainties need to be obtained. A subscale test program in the icing research cell R1D would provide a cost effective method of acquiring the necessary data. One of the principle weaknesses of this model is its reliance on empirical data from R1D to model the nozzle nearfield. Empirical turbulence data need to be obtained for the larger test cells as well since they have different spray systems. Until these questions are addressed, the ability to accurately predict flight icing conditions in an altitude test cell will be limited.

LIST OF REFERENCES

LIST OF REFERENCES

1. Bartlett, C. Scott "An Empirical Look at Tolerances in Setting Icing Test Conditions with Particular Application to Icing Similitude" AEDC-TR-87-23, August 1988.

2. Glass, Morton "Droplet Spectra and Liquid Water Content Measurements in Aircraft Icing Environments" American Meteorology Society Conference on Cloud Physics, November 1982.

3. Gall, E. S. and Floyd, F. X. "Icing Test Capability of the Engine Test Facility Propulsion Development Test Cell J-1" AEDC-TR-71-94, August 1971.

4. Bartlett, C. Scott "Icing Testing Cloud Simulation Requirements" AIAA Paper No. 89-0736, January 1989.

5. Willbanks, C. E. and Schultz, R. J. "Analytical Study of Icing Simulation for Turbine Engines in Altitude Test Cells" AEDC-TR-73-144, November 1973.

6. Lankford, D. W. "Icing Distribution Code: FASERSVT" AEDC Unpublished User's Manual, September 1986.

7. "Airworthiness Standards; Transport Category Airplanes: Appendix C", Federal Aviation Regulations, Part 25, Federal Aviation Administration, January 1984.

8. Shuen, J. S.; Solomon, A. S. P.; Zhang, Q. F. and Faeth, G. M. "A Theoretical and Experimental Study of Turbulent Particle-Laden Jets" NASA CR-168293, November 1983.

9. Faeth, G. M. "Recent Advances in Modeling Particle Transport Properties and Dispersion in Turbulent Flow" ASME/JSME Thermal Engineering Joint Conference, 1983.

10. Sturgess, G. S.; Syed, S.A. and McManus, K.R. "Calculation of a Hollow-Cone Liquid Spray in a Uniform Air Stream" AIAA Paper No. 84-1322, June 1984.

11. Nichols, Robert H. "The Effect of Particle Dynamics on Turbulence Measurements with the Laser Doppler Velocimeter" PhD Dissertation UTSI, June 1986.

12. Holman, J. P. "Experimental Methods for Engineers" McGraw-Hill Book Company, 1984.

13. Oberkampf, William L "Synergism of Computational Aerodynamics and Wind Tunnel Experiments" AEDC Technical Seminar Program, April 1989.

14. Hovenac, Edward A "Calibration of Droplet Sizing and Liquid Water Content Instruments: Survey and Analysis" NASA CR-175049, May 1986.

15. "Power Test Codes: Flow Measurement" ASME Instruments and Apparatus Supplement, February 1959.

16. Beyer, William H. "CRC Standard Mathematical Tables" CRC Press, Inc., 1984.

APPENDIXES

APPENDIX A
Figures

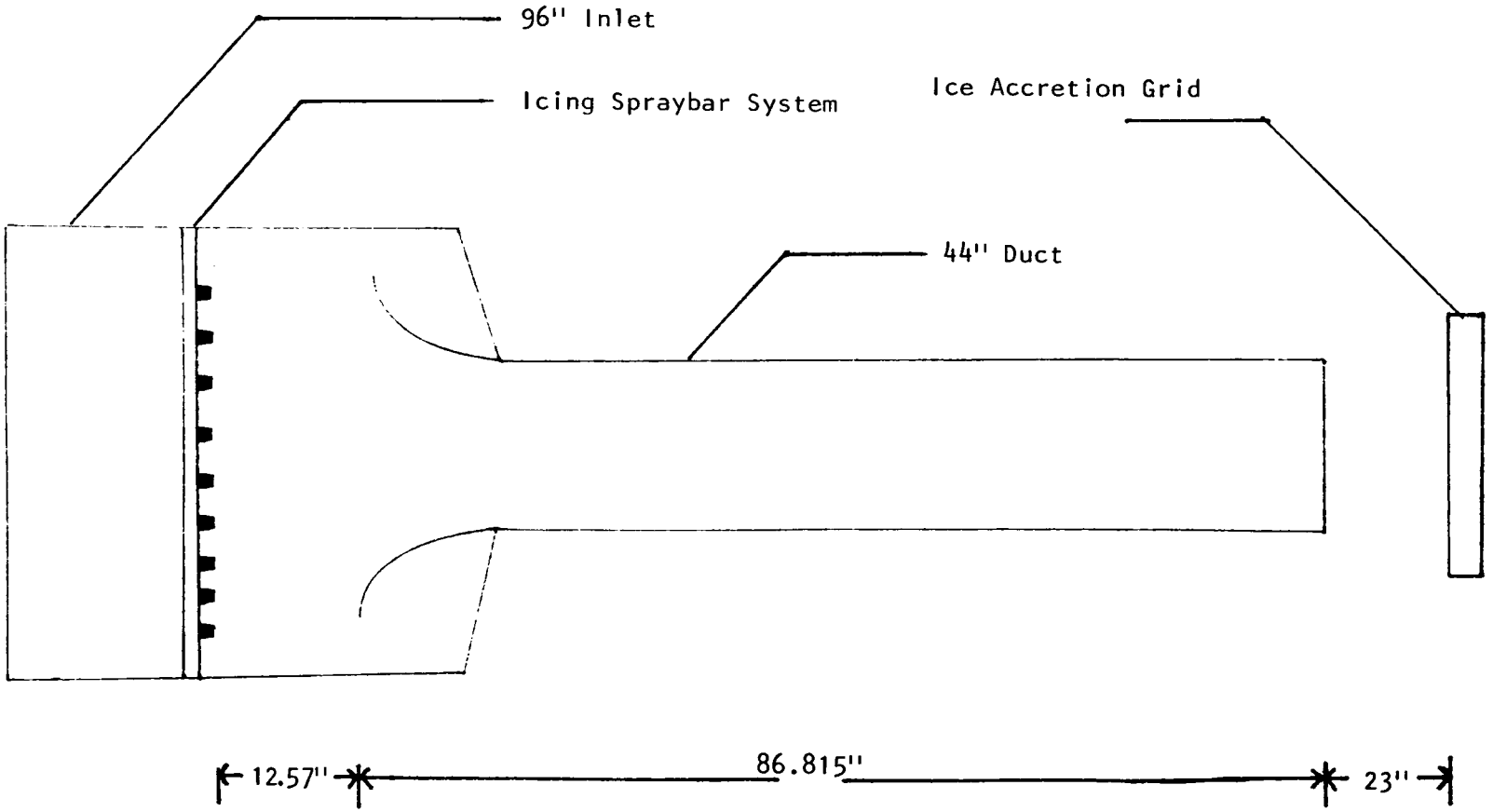
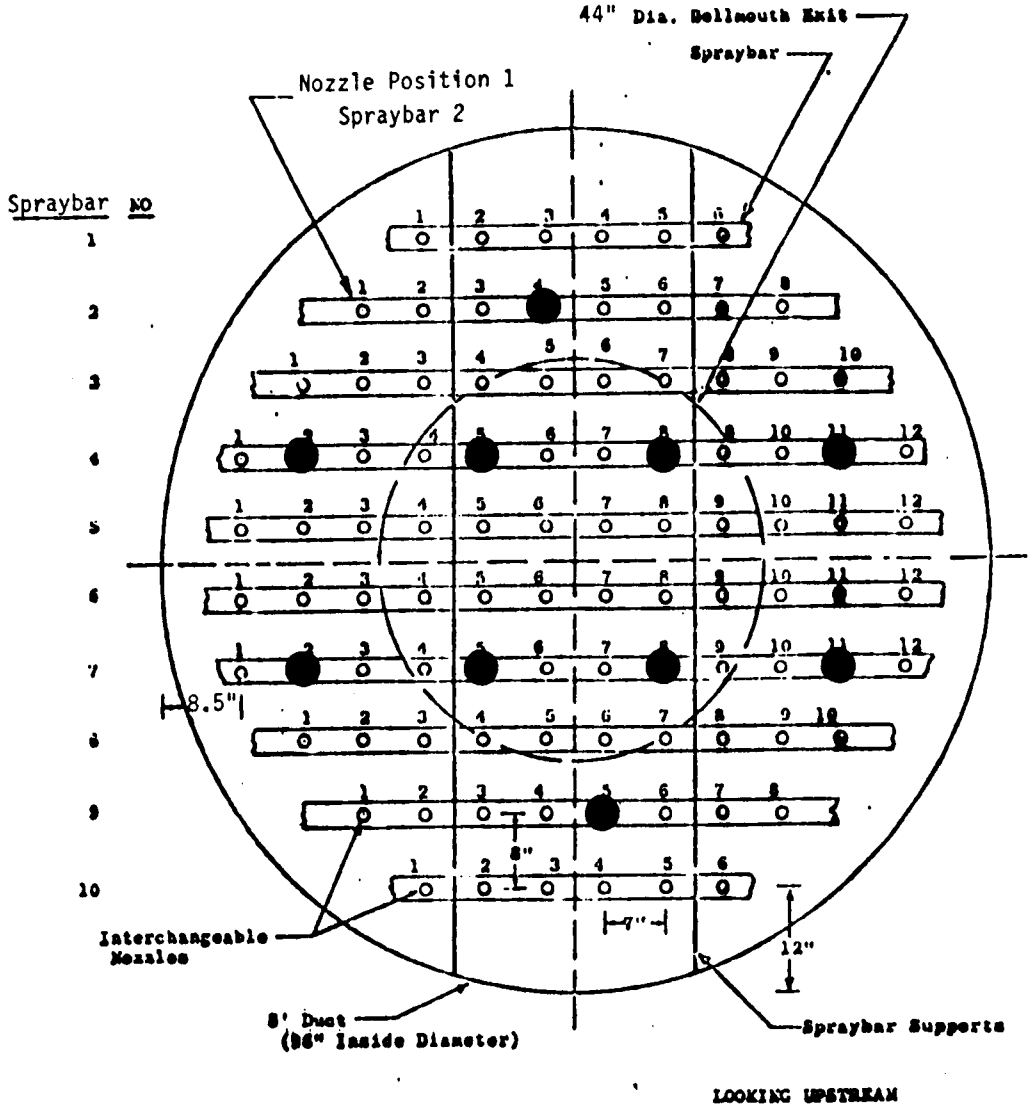


Figure 1. J-1 Icing Calibration System



ICING TEST SPRAYBAR ASSEMBLY

Figure 2. Baseline Nozzle Location

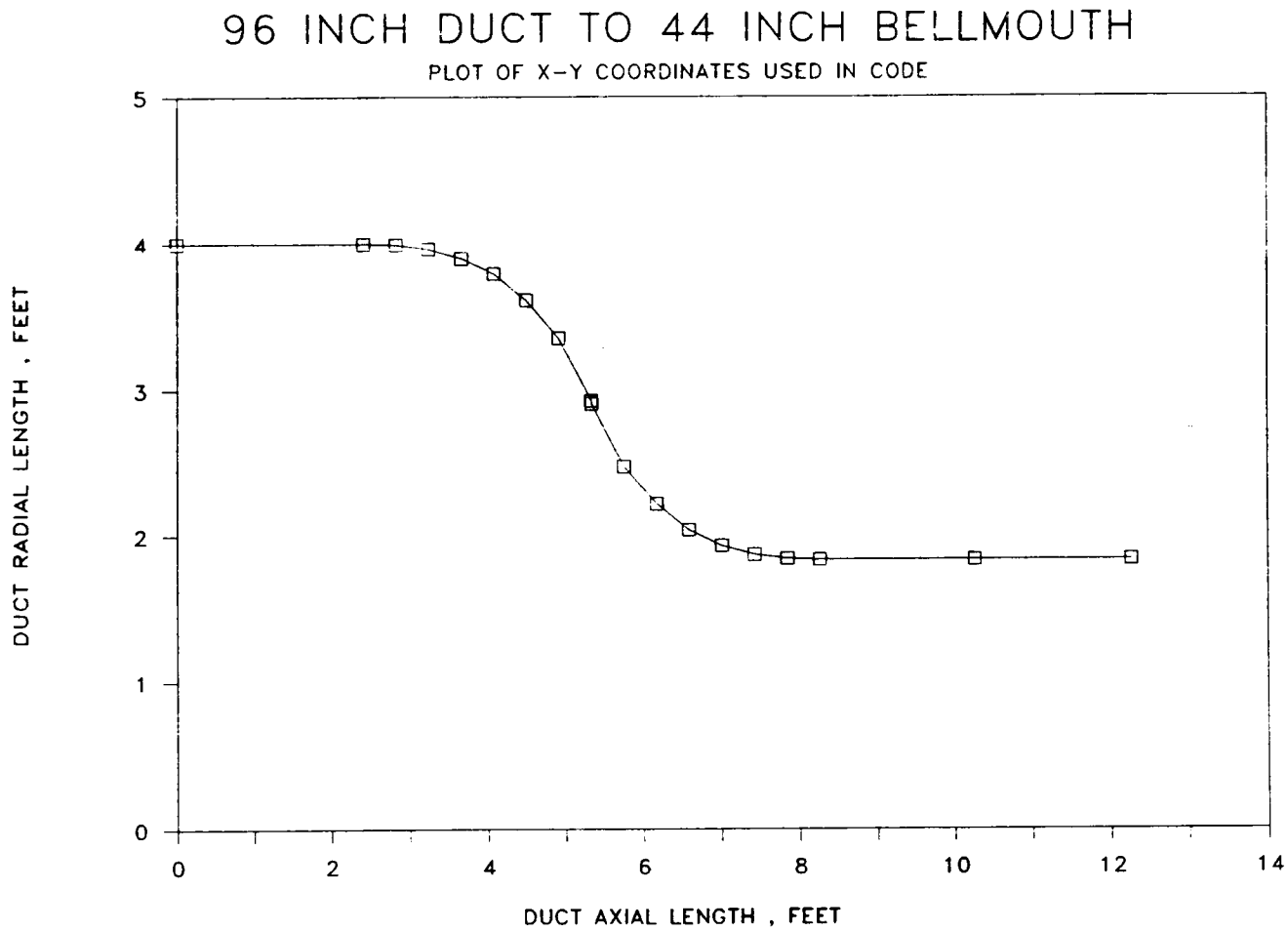


Figure 3. Baseline Bellmouth (e = .93)

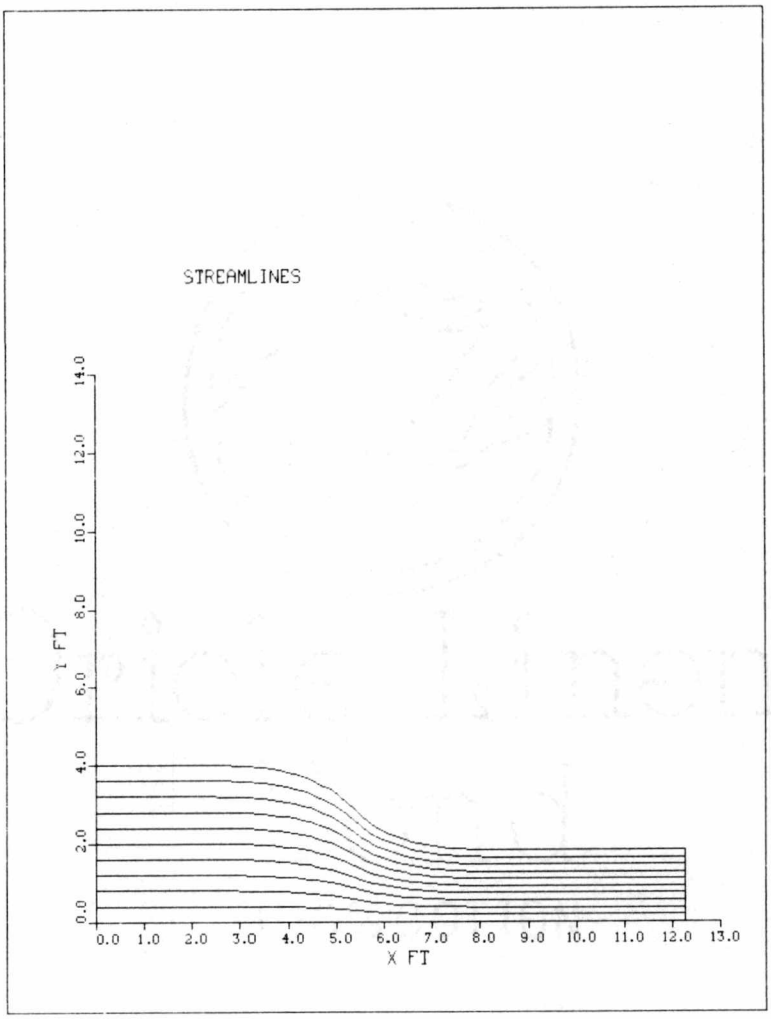


Figure 4. J-1 Streamline Plot

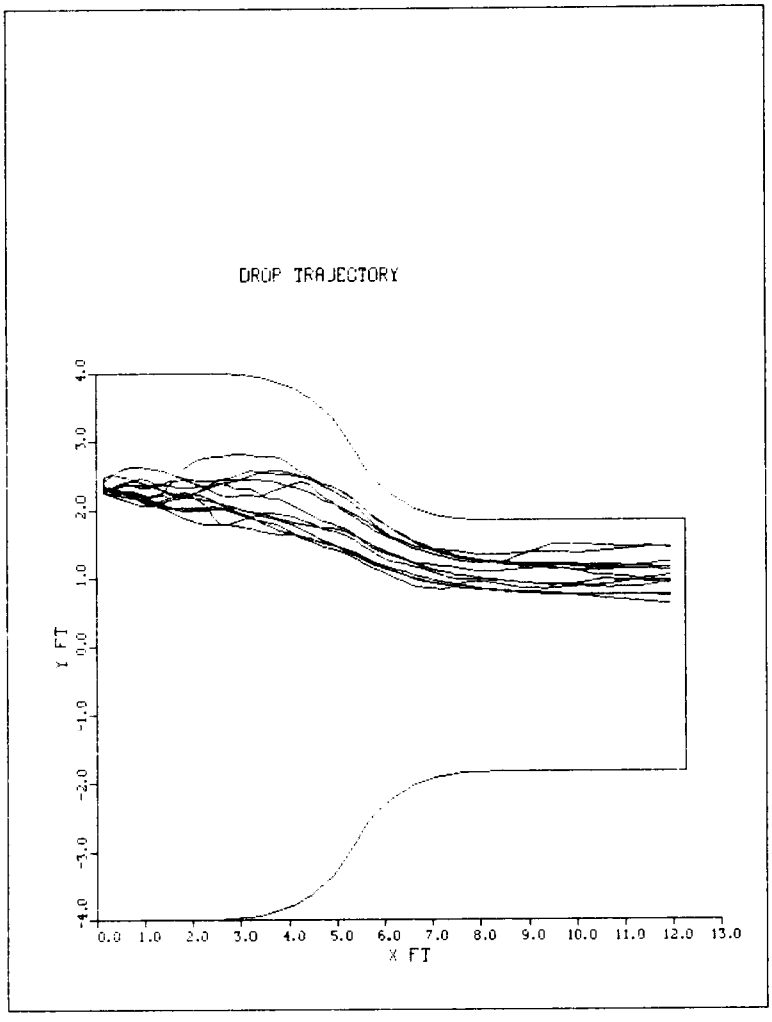


Figure 5. J-1 Trajectory Plot

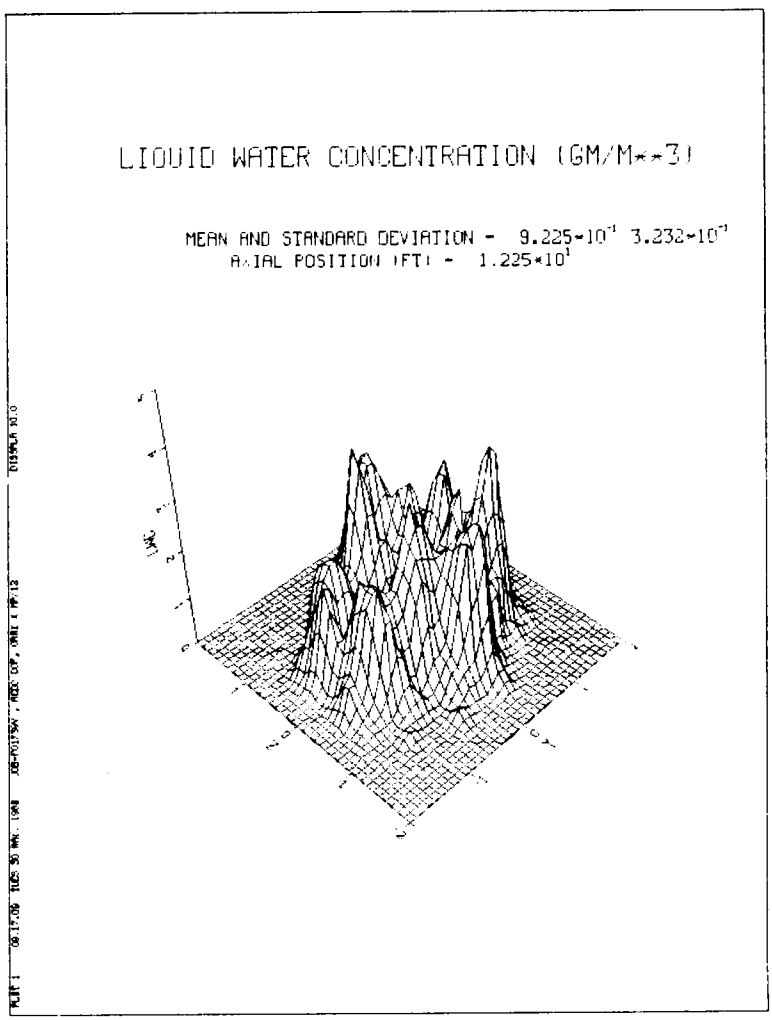


Figure 6. J-1 Topographical Plot of LWC

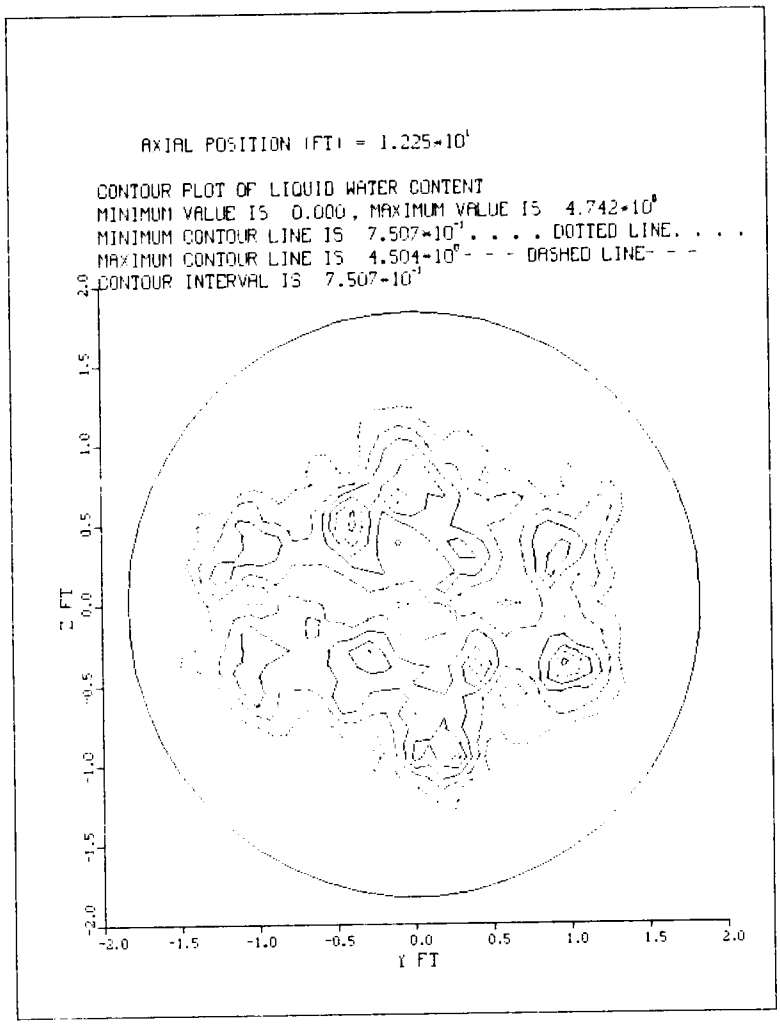


Figure 7. J-1 Contour Plot of LWC

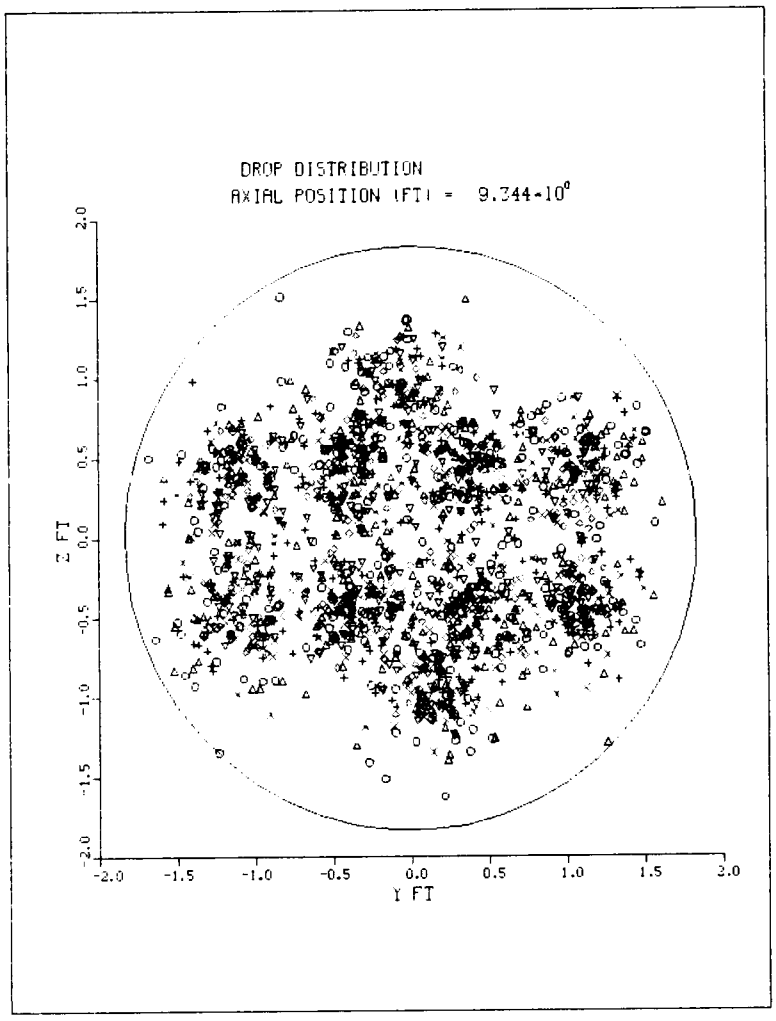


Figure 8. J-1 Drop Distribution Plot 9.344 ft Downstream of Spraybars

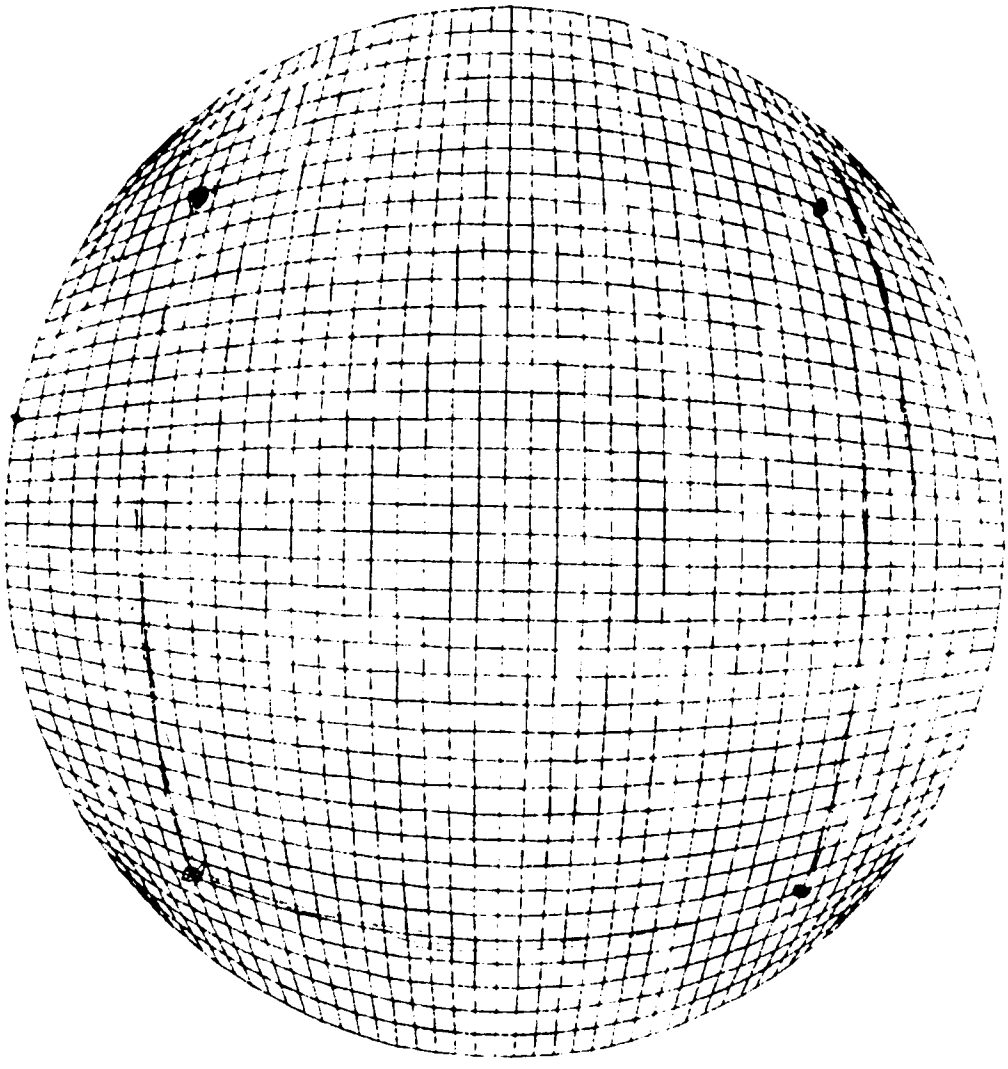


Figure 9. Grid Elements in J-1 Ducting

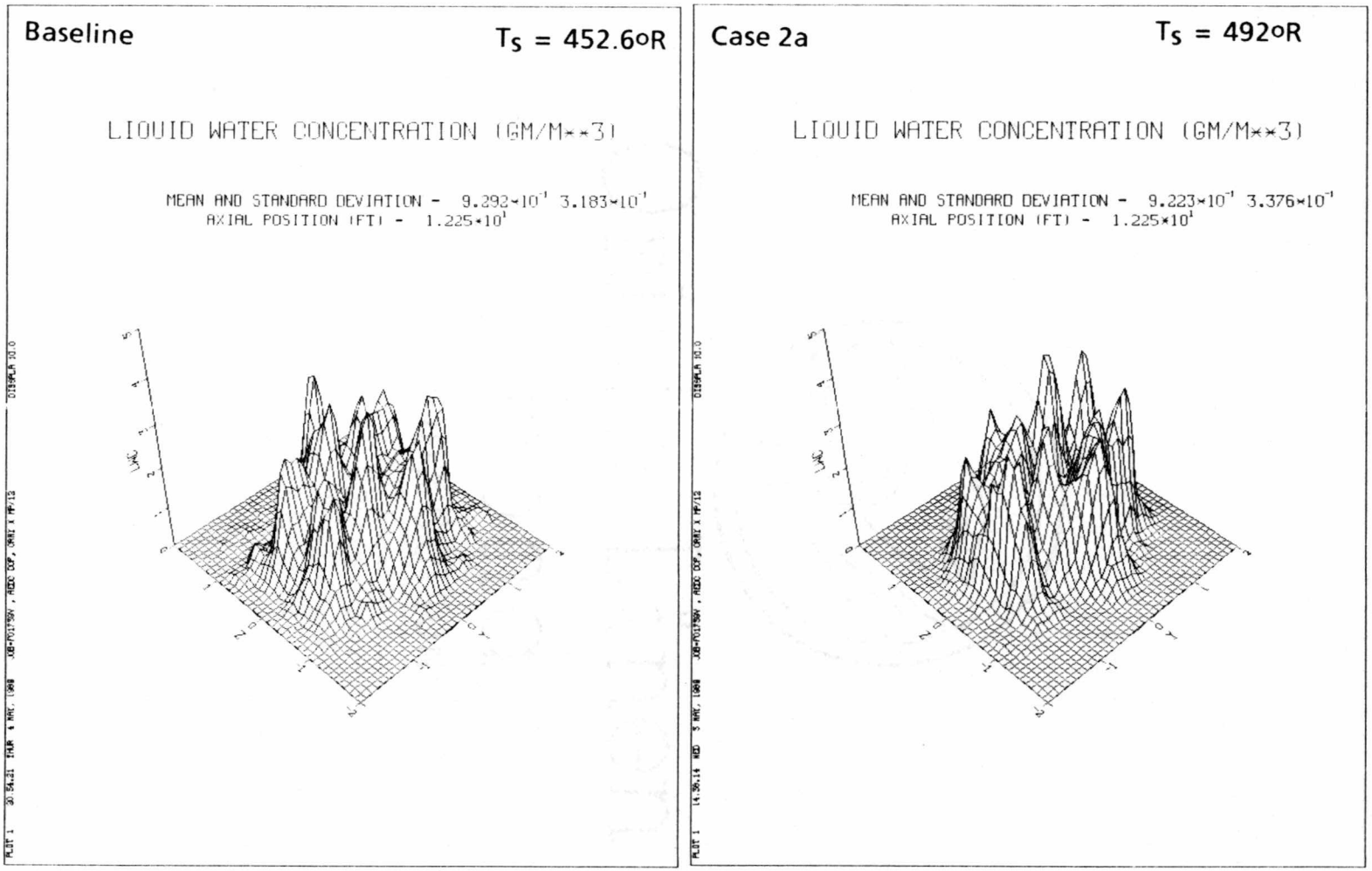


Figure 10. Comparison of LWC Distributions Obtained for the Baseline Case and Case 2a with Increased Static Temperature

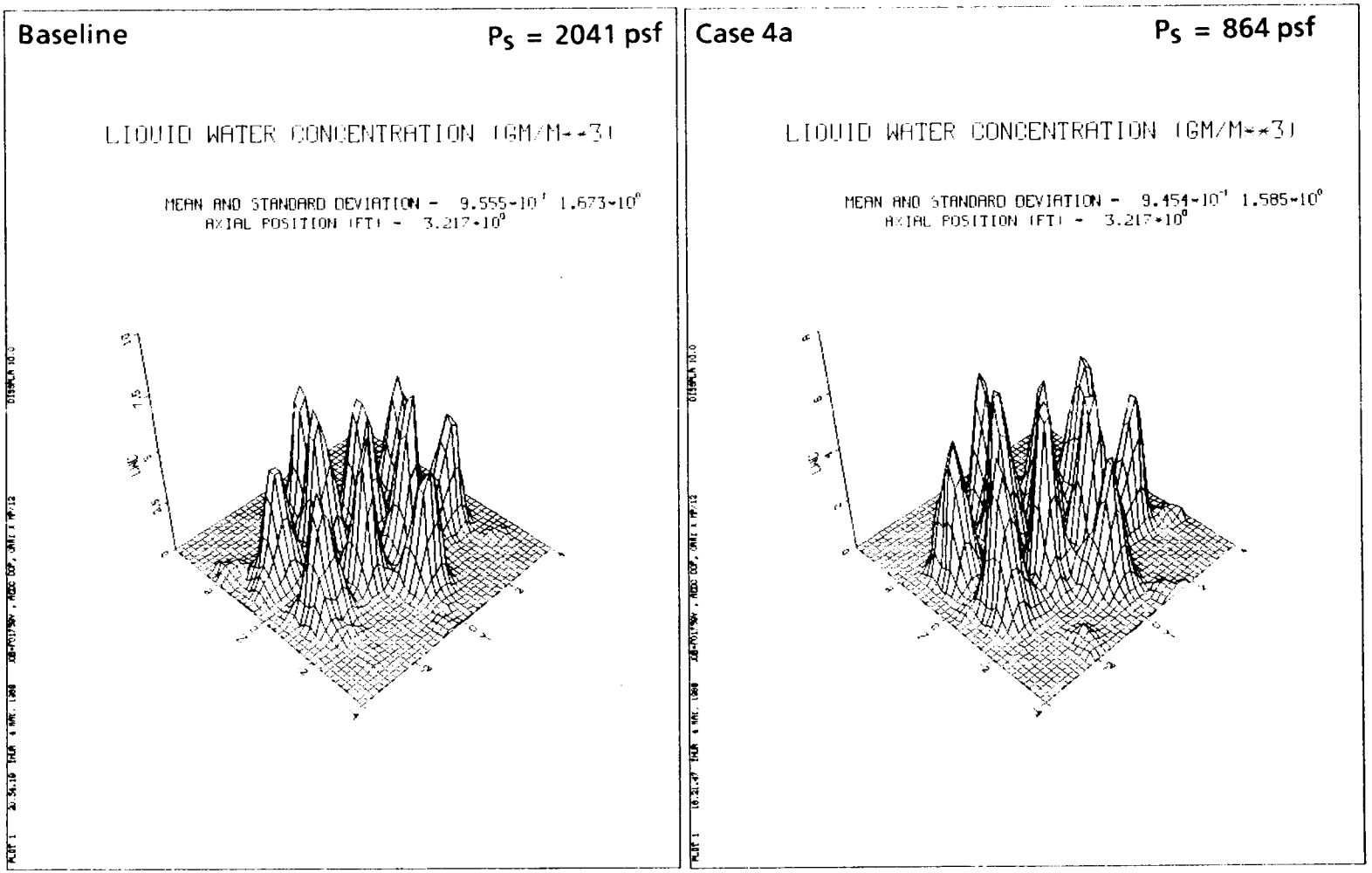


Figure 11. Comparison of LWC Distributions Obtained for the Baseline Case and Case 4a with Decreasing Static Pressure at 3.217 ft.

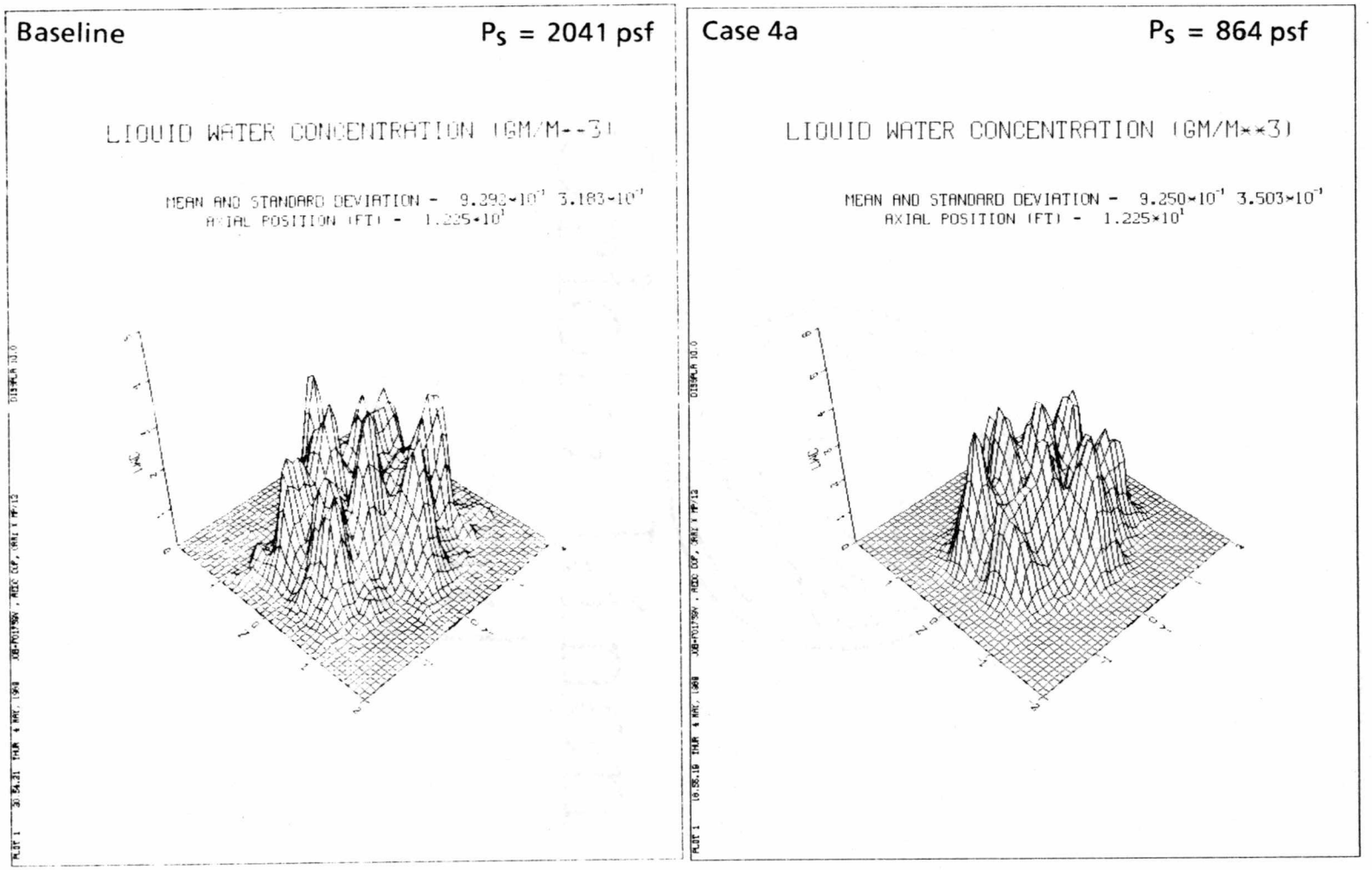


Figure 12. Comparison of LWC Distributions Obtained for the Baseline Case and Case 4a with Decreasing Static Pressure at 12.25 ft.

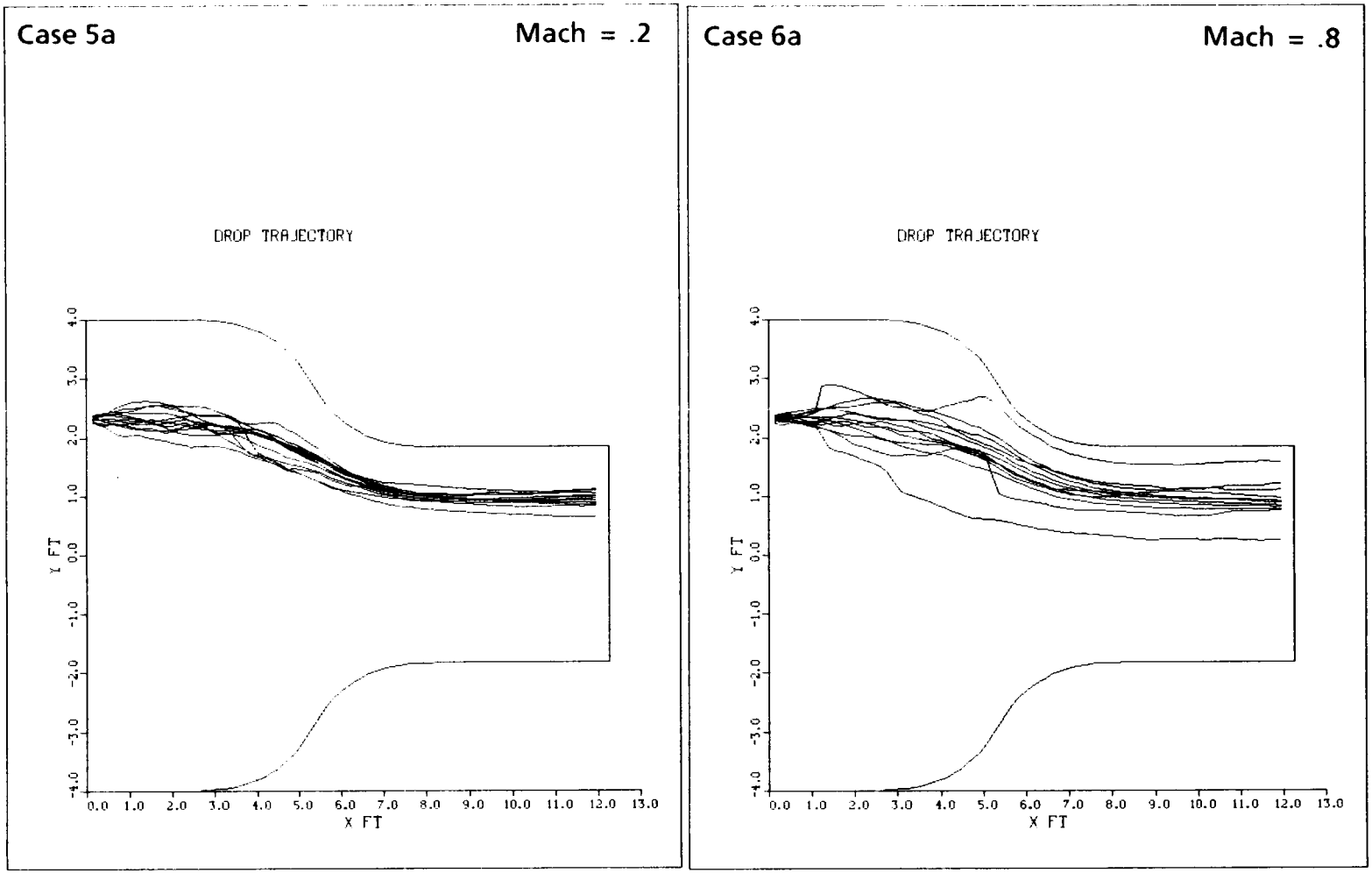


Figure 13. Comparison of Drop Trajectory Plots for Cases 5a and 6a with Increasing Mach Number

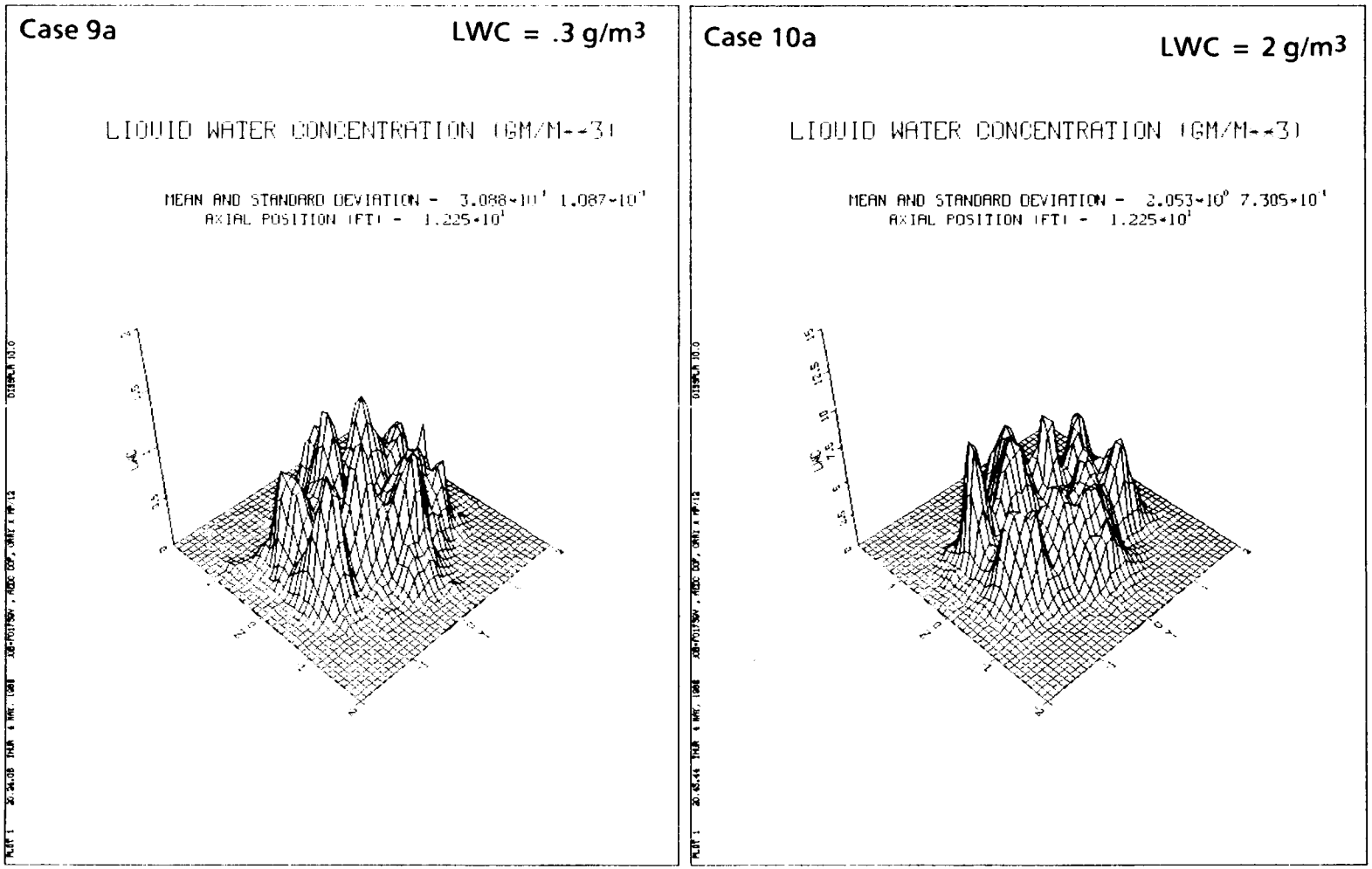


Figure 14. Comparison of LWC Distributions Obtained for Cases 9a and 10a While Varying Bulk LWC

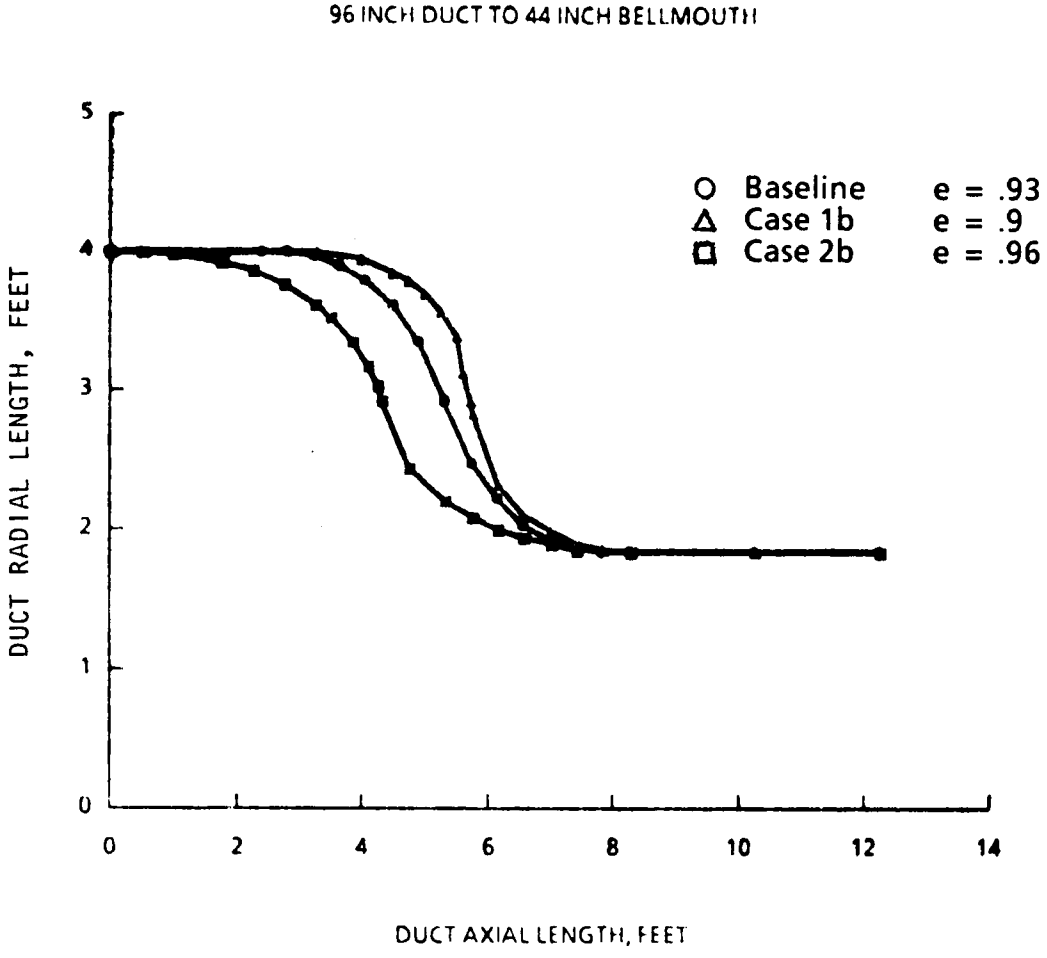
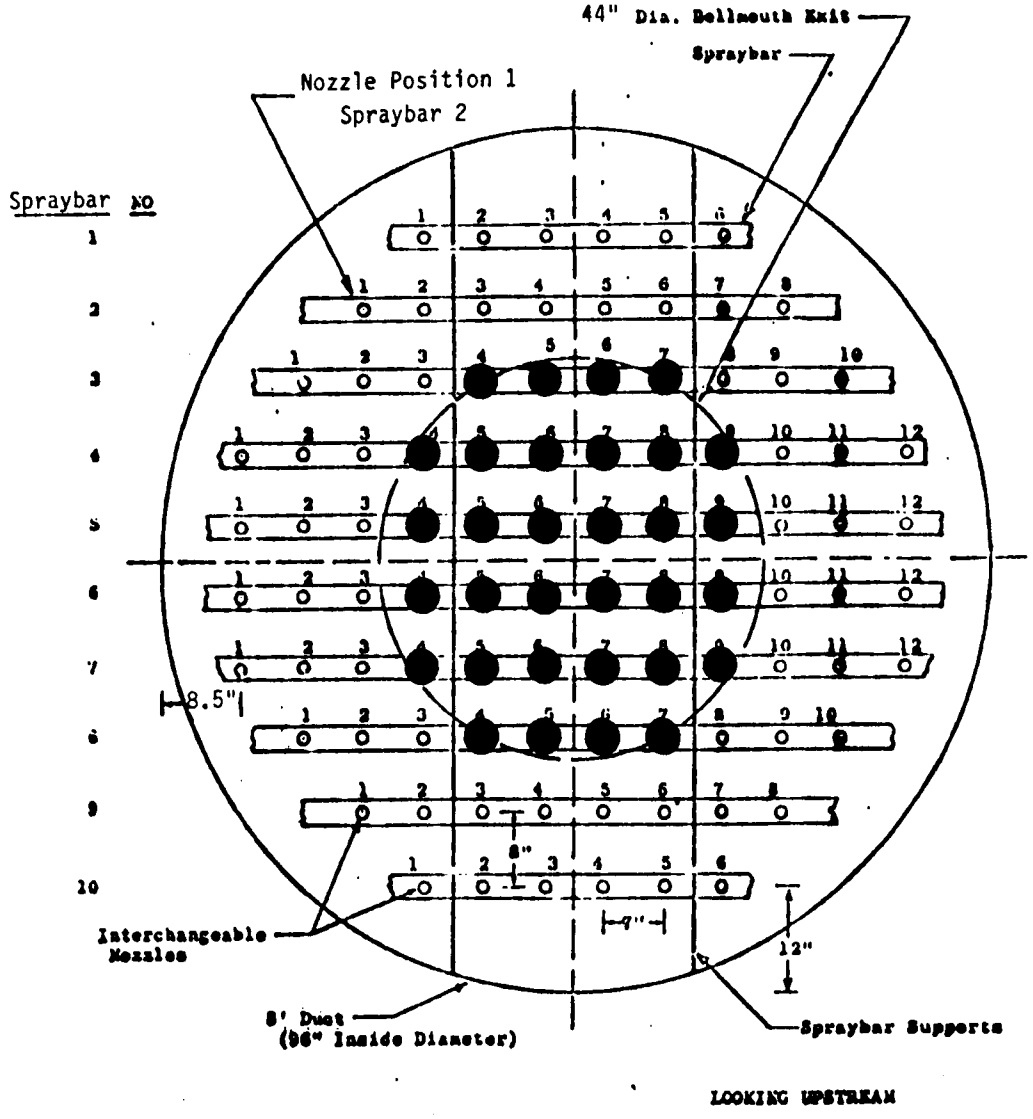
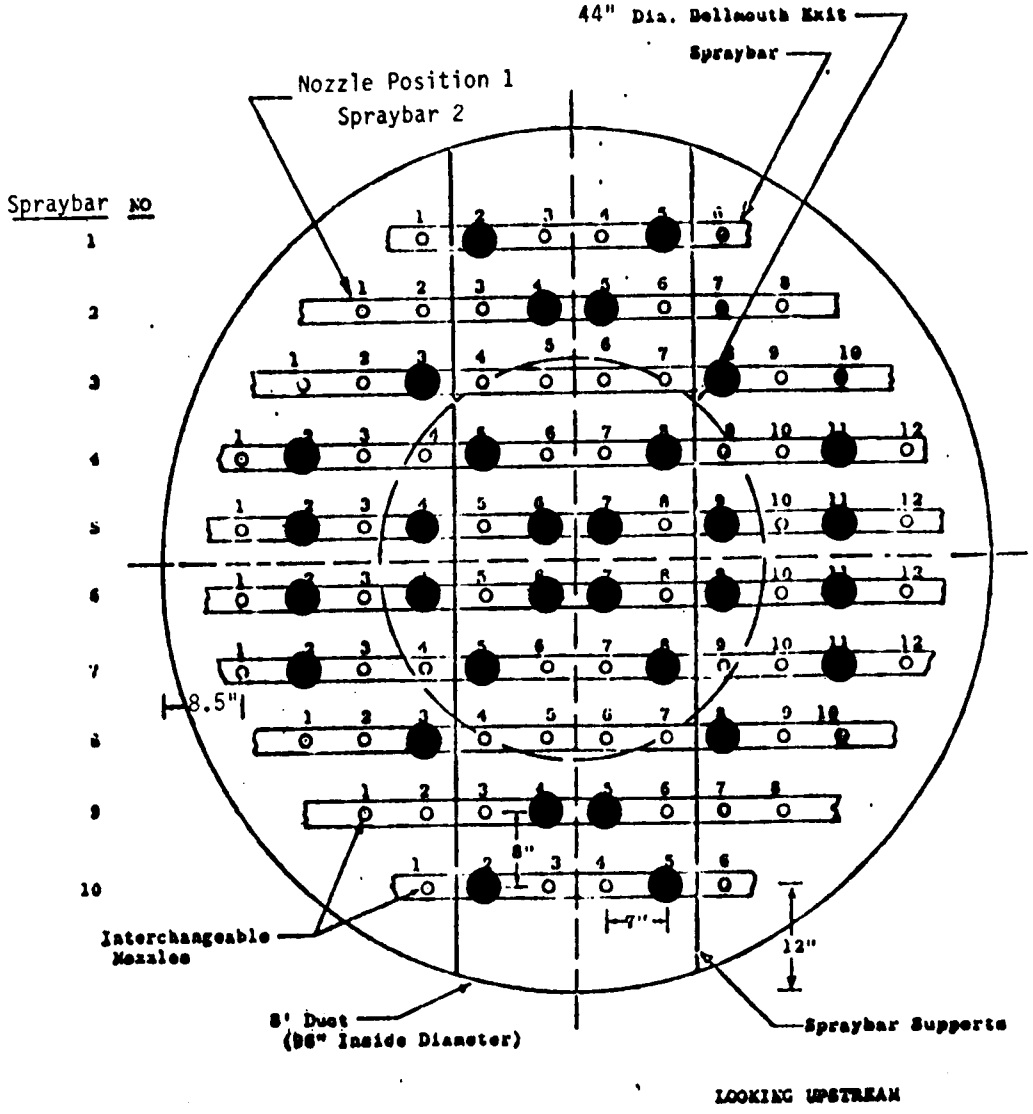


Figure 15. Bellmouth Curvature for Different Eccentricities



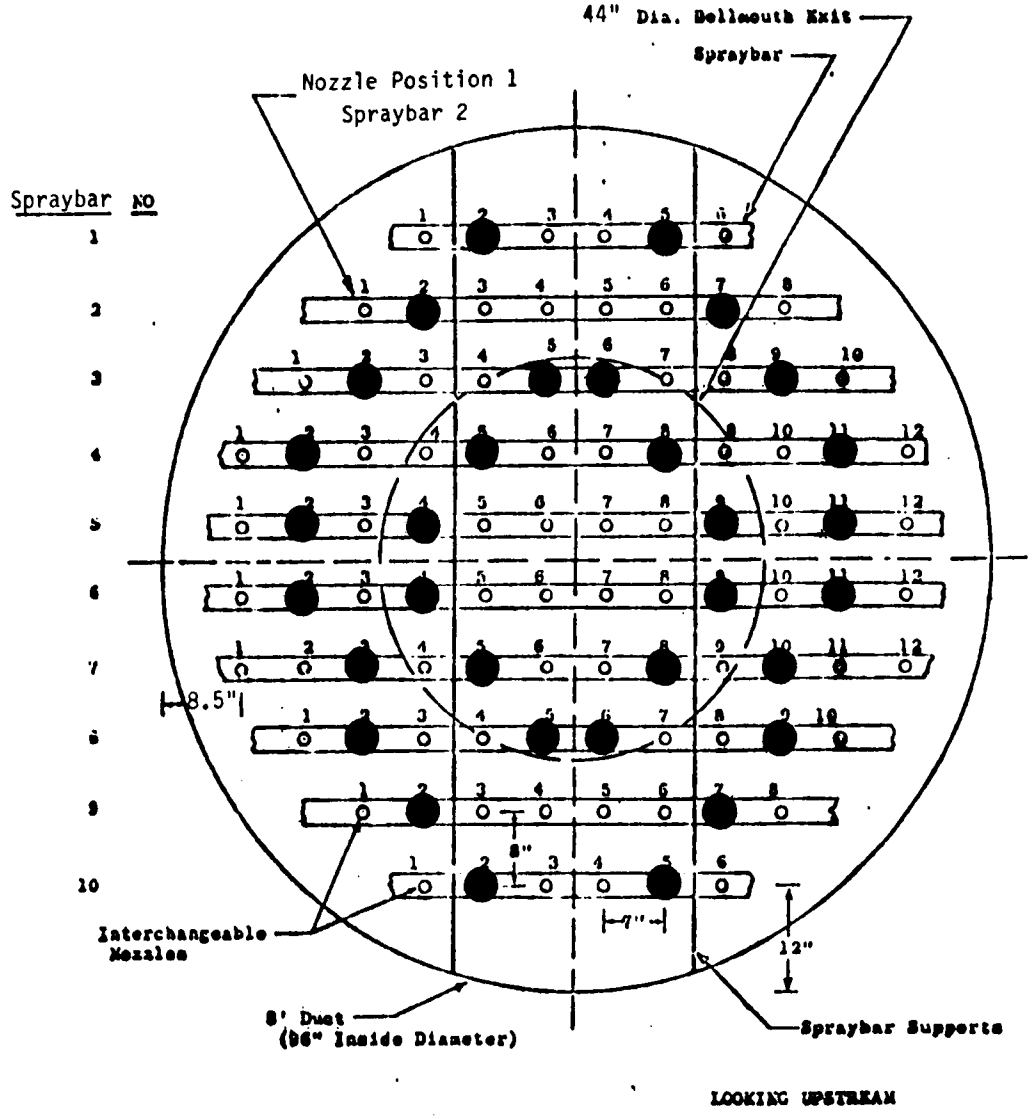
ICING TEST SPRAYBAR ASSEMBLY

Figure 16. Case 7b Nozzle Location (Inward)



ICING TEST SPRAYBAR ASSEMBLY

Figure 17. Case 4b Nozzle Location (Even)



ICING TEST SPRAYBAR ASSEMBLY

Figure 18. Case 6b Nozzle Location (Outward)

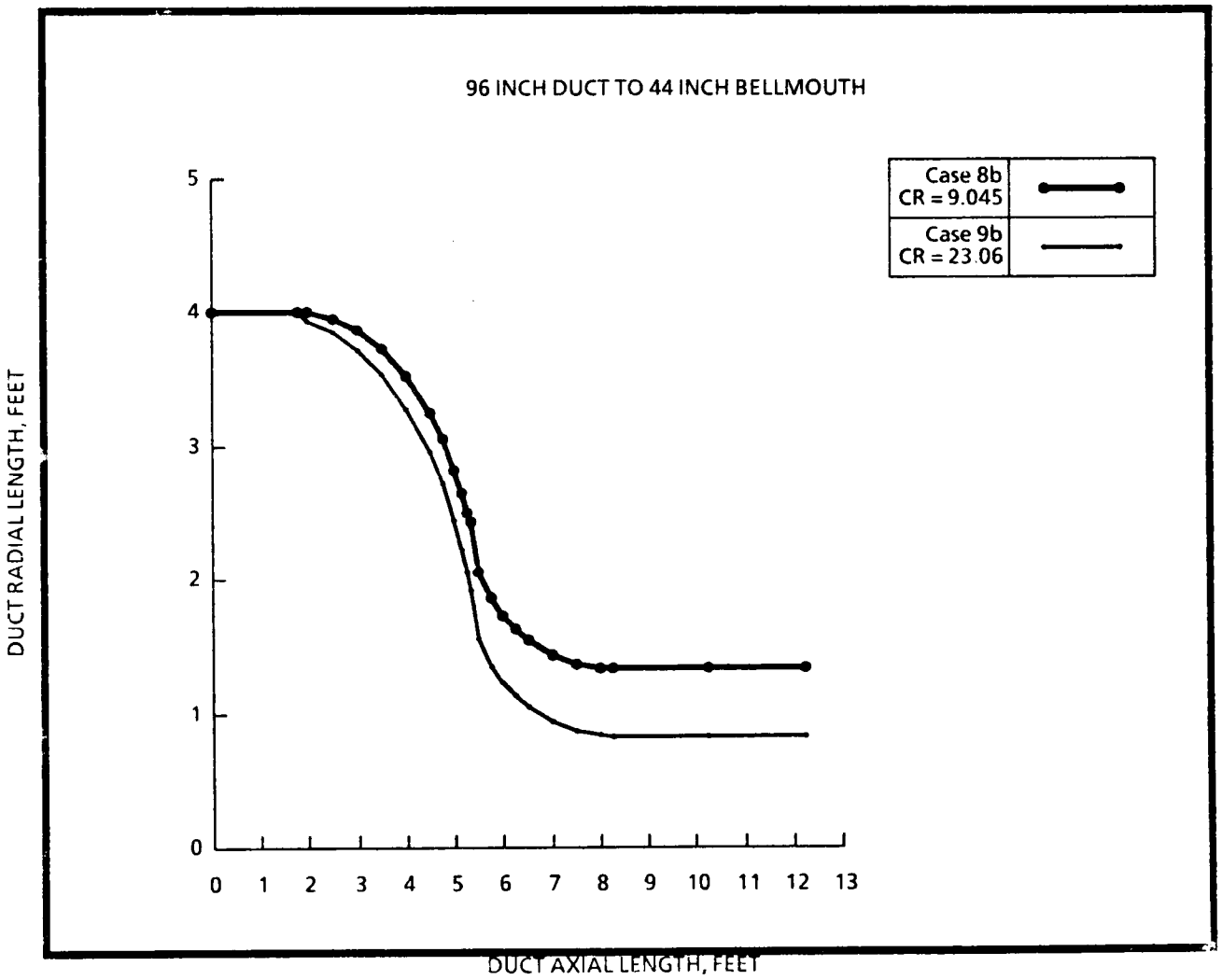
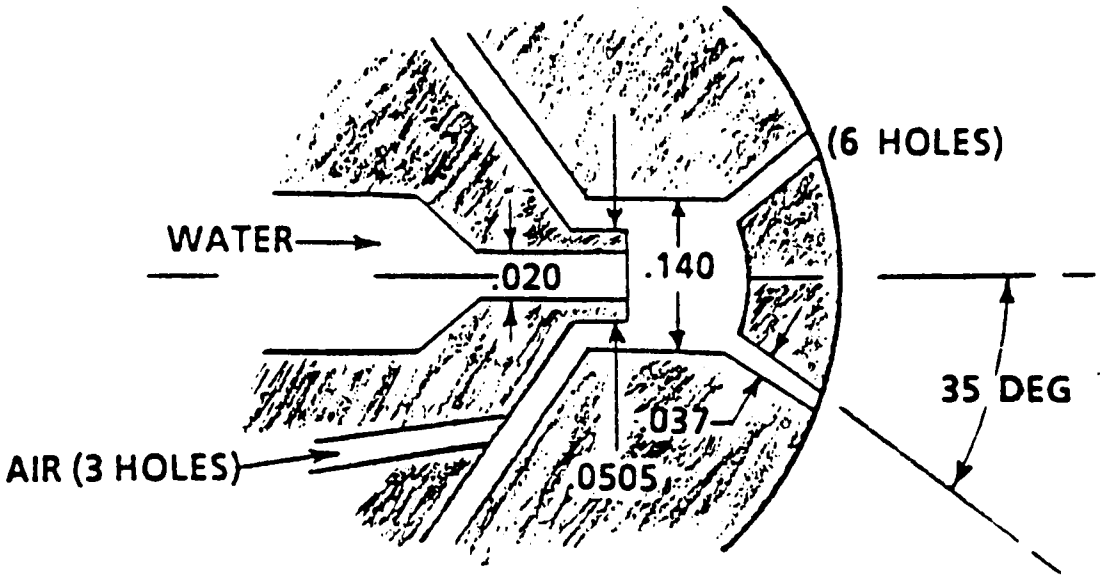


Figure 19. Area Contraction Ratio Variation



DIMENSIONS IN INCHES

Figure 20. AEDC 2050 Spray Nozzle

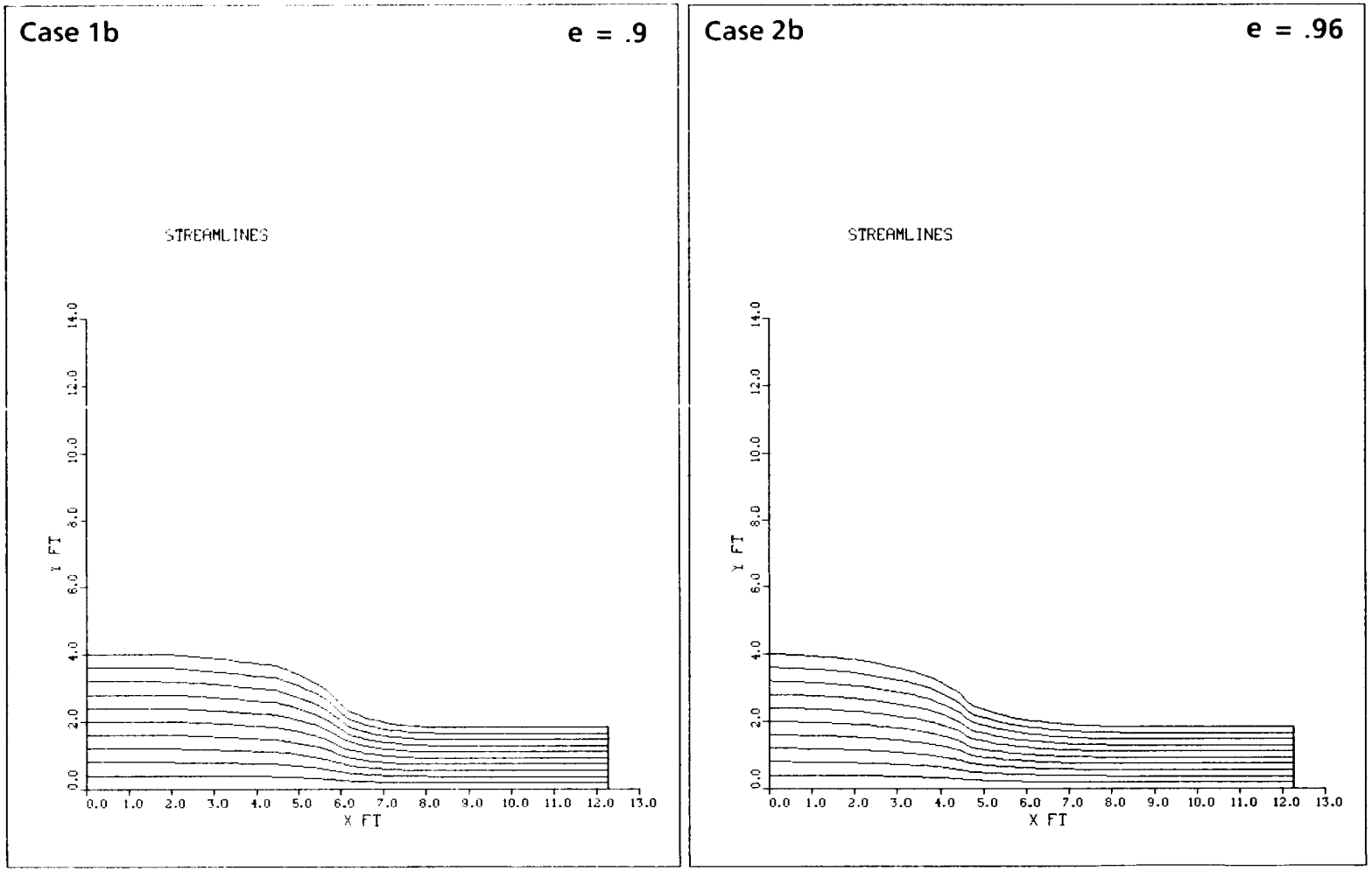


Figure 21. Comparison of Streamlines for Cases 1b and 2b Obtained While Increasing Eccentricity

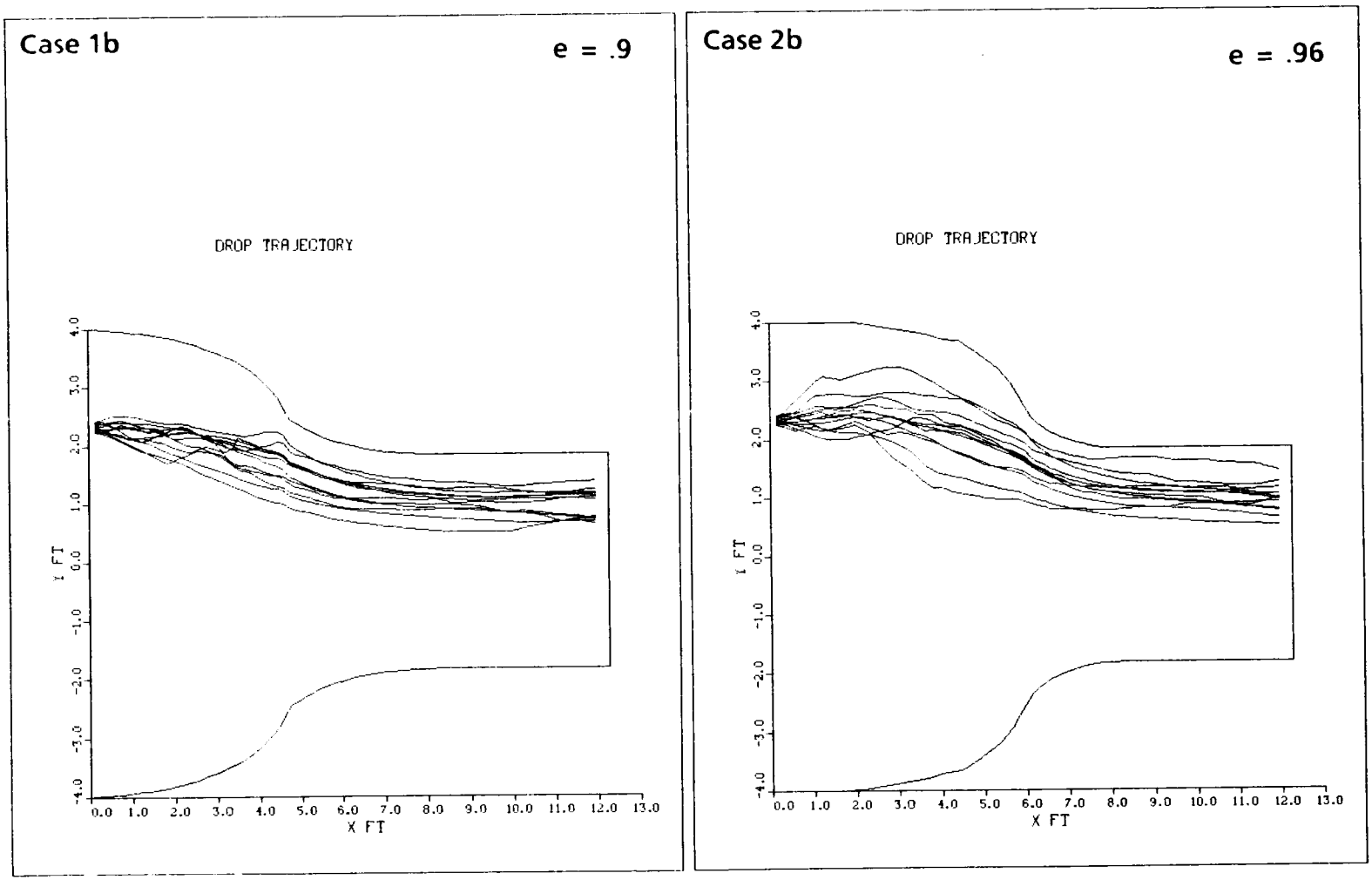


Figure 22. Comparison of Drop Trajectory Plots for Cases 1b and 2b Obtained While Increasing Eccentricity

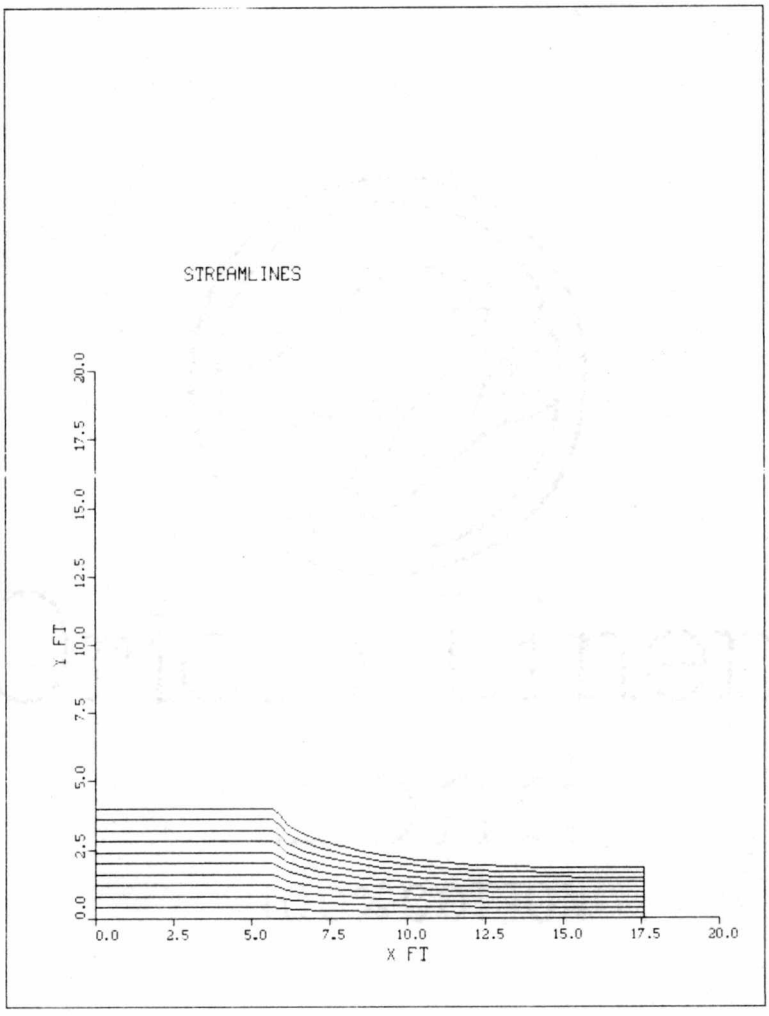


Figure 23. Case 3b Streamlines for Eccentricity of .97

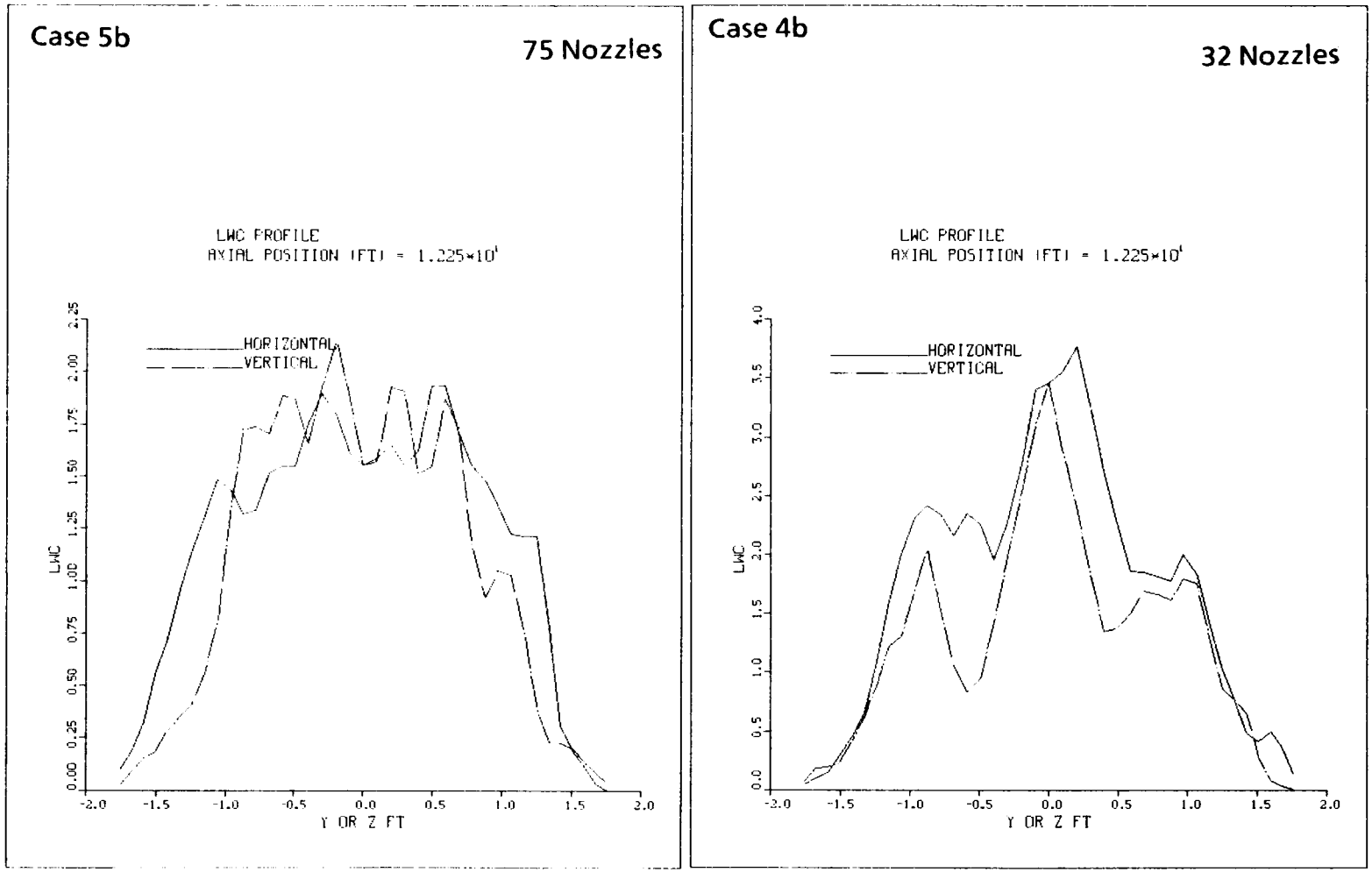


Figure 24. Comparison of LWC Profiles for Cases 4b and 5b While Increasing the Number of Nozzles

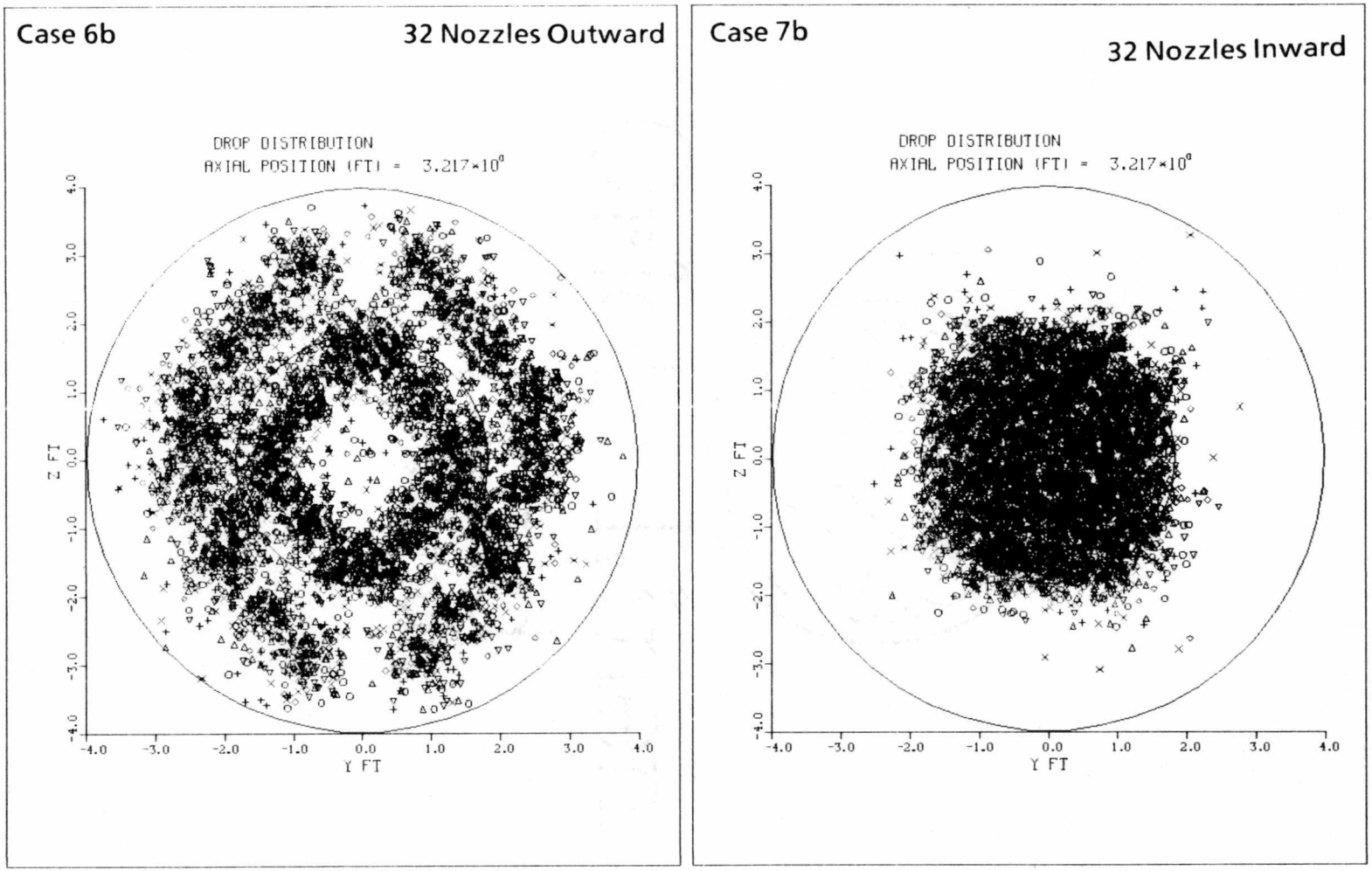


Figure 25. Drop Distribution at 3.217 ft. for Different Nozzle Locations

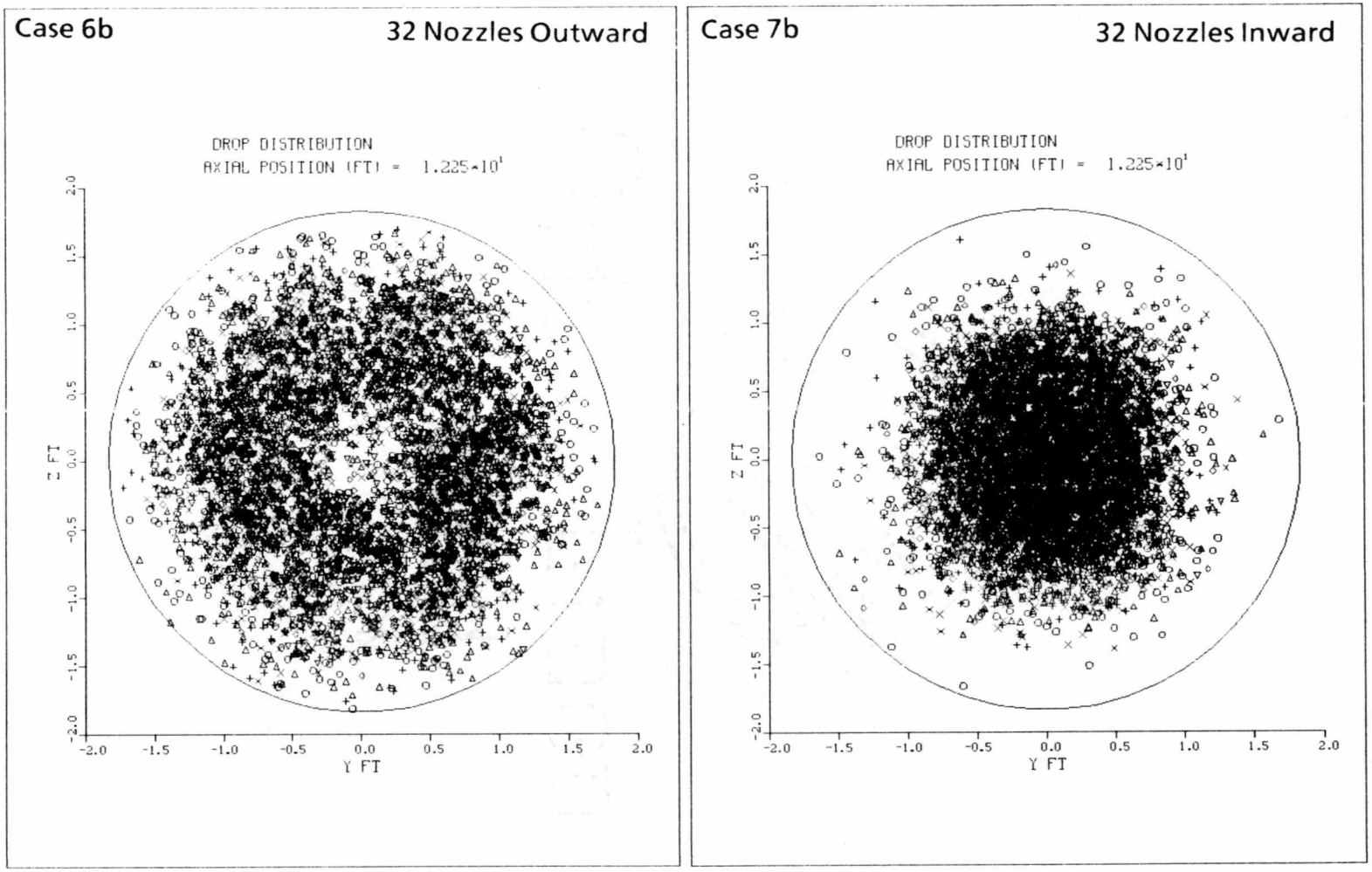


Figure 26. Drop Distribution at 12.25 ft. for Different Nozzle Locations

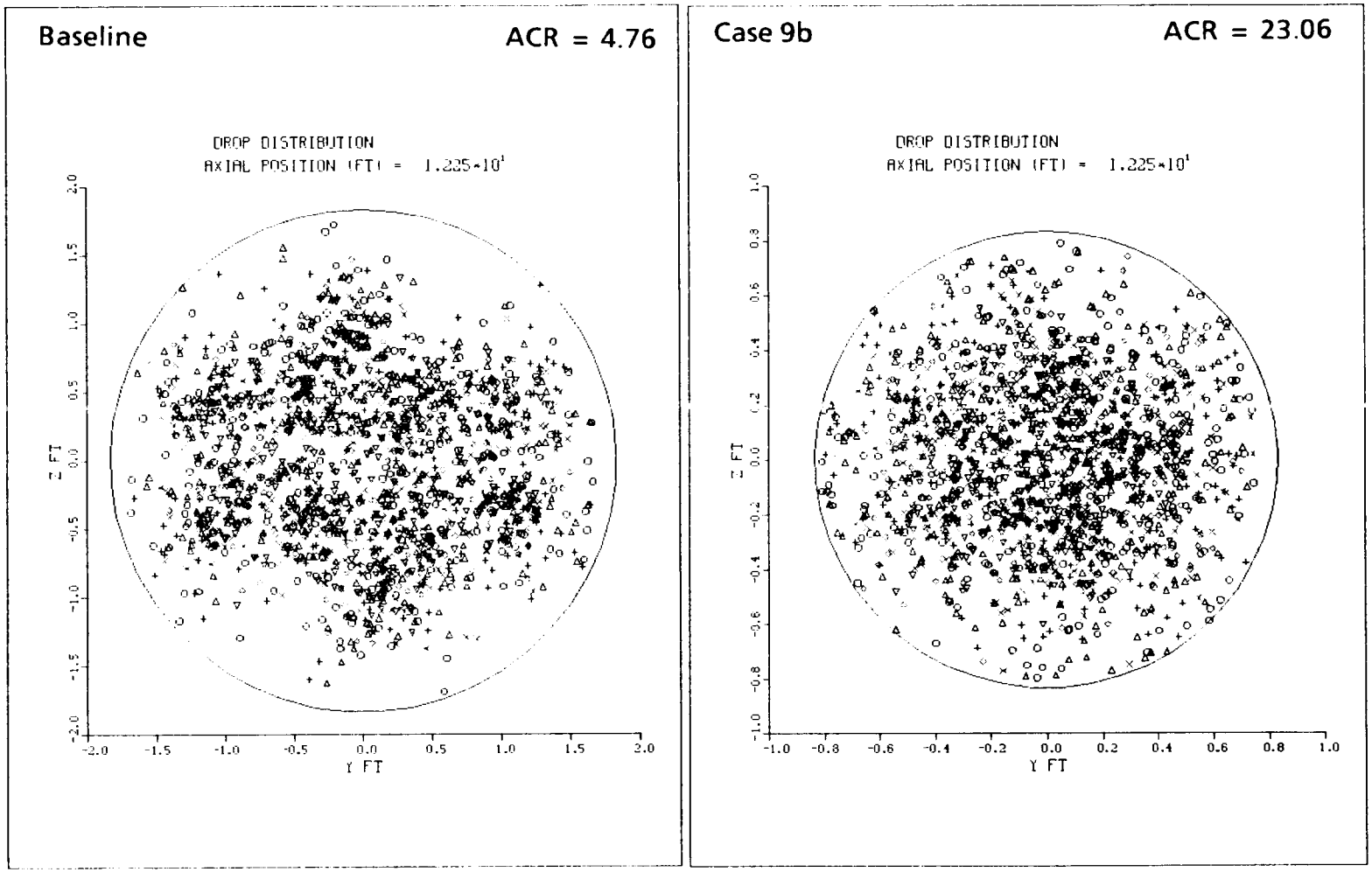


Figure 27. Drop Distribution for Different Area Contraction Ratios

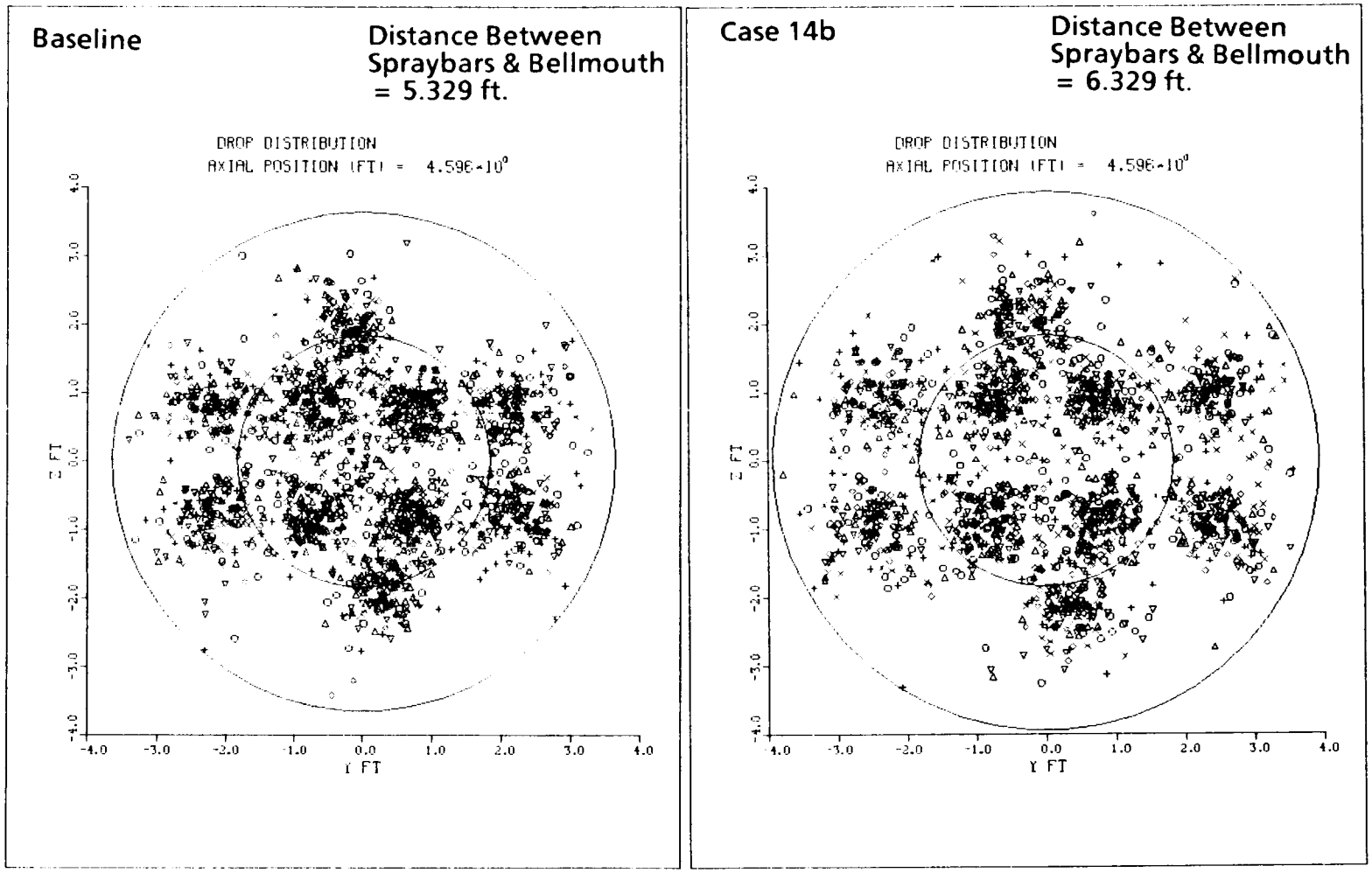


Figure 28. Drop Distribution for Different Bellmouth to Spraybar Lengths

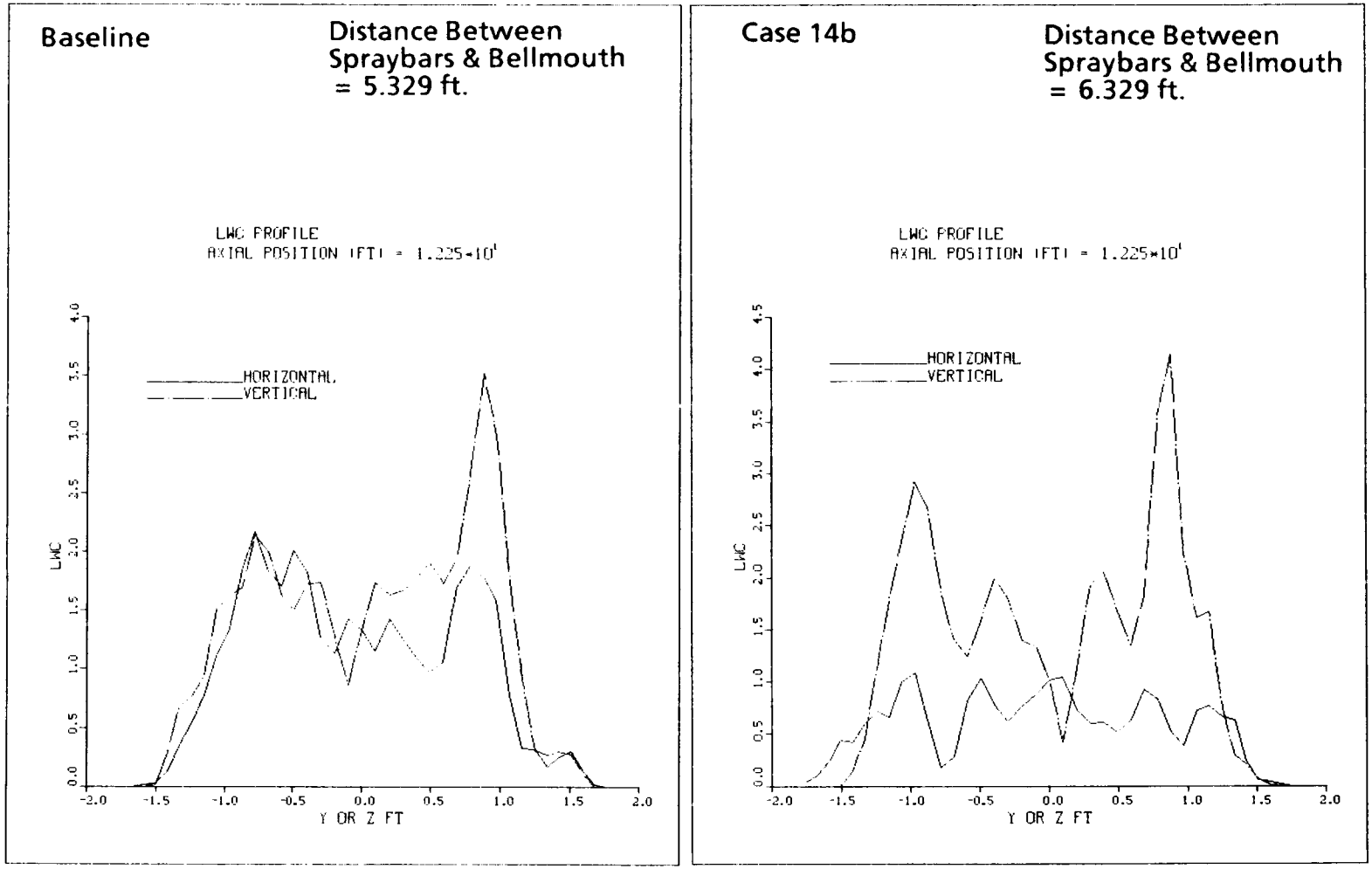


Figure 29. LWC Profiles for Different Bellmouth to Spraybar Lengths

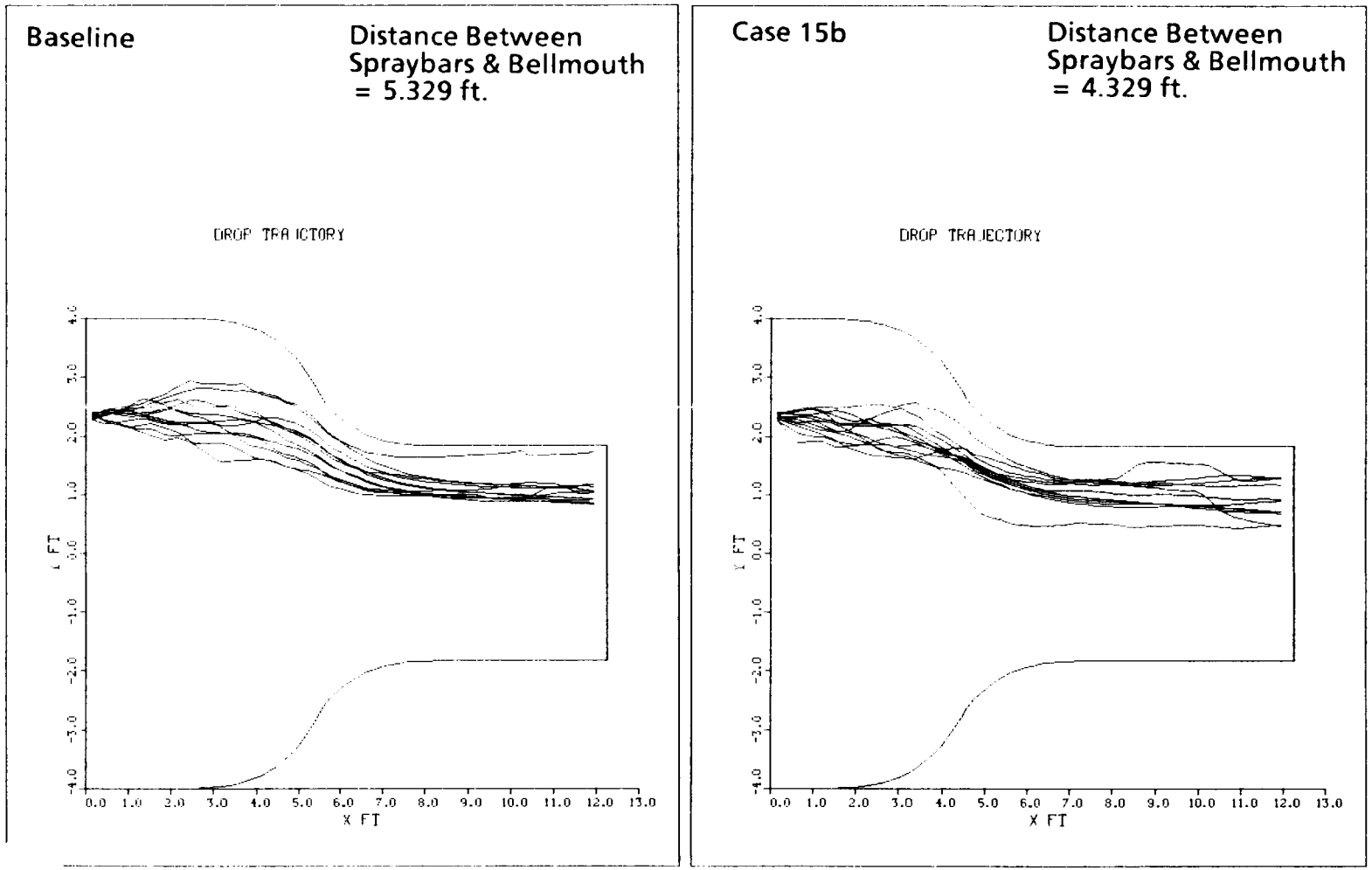


Figure 30. Drop Trajectory for Different Bellmouth to Spraybar Lengths

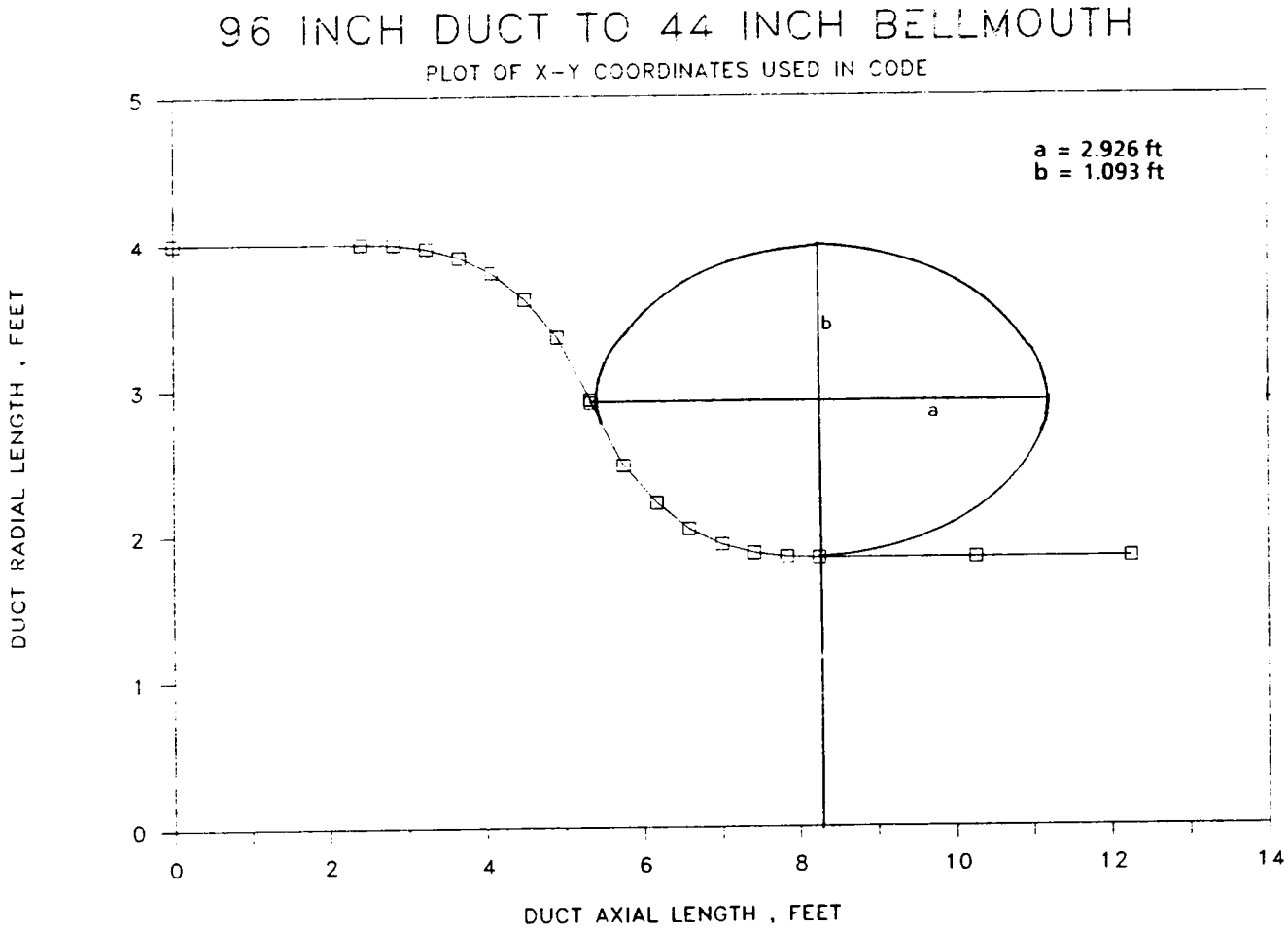


Figure 31. Baseline Ellipse

APPENDIX B
Tables

TABLE 1

BASELINE DIFFERENCES

CASE #	SIGMA	PERCENT DIFFERENCE FROM ORIGINAL BASELINE
ORIGINAL BASELINE	.3183	--
1a	.3332	-4.68%
2a	.3297	-3.58%
3a	.3316	-4.17%
4a	.3257	-2.32%
5a	.3307	-3.9%
6a	.3232	-1.5%
7a	.3317	-4.2%
8a	.3374	-6.0%
9a	.3230	-1.4%
10a	.3212	-0.9%
BASELINE AVERAGE	.3278	

TABLE 2

METEOROLOGICAL PARAMETERS AND CODE INPUT
(Changes From Baseline)

CASE #	PARAMETER VARIED	CODE INPUT
1a	STATIC TEMP (438 DEG R)	TINF = 463.4 WC = .0401
2a	STATIC TEMP (492 DEG R)	TINF = 520.5 WC = .0424
3a	STATIC PRES (2116.8 PSF)	PINF = 2581.5
4a	STATIC PRES (864 PSF)	PINF = 1054
5a	MACH (= .2)	FSMACH = .042 WC = .0148 PINF = 2096 TINF = 456
6a	MACH (= .8)	FSMACH = .12 WC = .0594 PINF = 3080 TINF = 509
7a	MDD (= 16.1 MICRONS)	DPOP = .165, .090, .055, .023, .019, .012
8a	MDD (= 25.9 MICRONS)	DPOP = .1, .075,.035, .033, .032, .023
9a	LWC (= .3 G/M^3)	WC = 60*.0136
10a	LWC (= 2.0 G/M^3)	WC = 60*.0907

TABLE 3

METEOROLOGICAL PARAMETRIC STUDY
STANDARD DEVIATION COMPARISON

CASE #	STANDARD DEVIATION OF LWC	% DIFFERENCE FROM BASELINE
BASELINE(avg)	.3278	--------
1a (T = 438)	.3212	2.0%
2a (T = 492)	.3376	-3.0%
3a (P = 2116.8)	.3281	-0.1%
4a (P = 864)	.3503	-6.86%
5a (M = .2)	.3264	0.40%
6a (M = .8)	.3257	0.60%
7a (MDD = 16.1)	.3529	-7.65%
8a (MDD = 25.9)	.3677	-12.17%
9a (LWC = .3)	.1087	66.84%
10a (LWC = 2.0)	.7305	-122.85%

TABLE 4

TEST CELL CONFIGURATION
PARAMETRIC STUDY

CASE #	STANDARD DEVIATION	PERCENT DIFFERENCE FROM BASELINE
BASELINE (AVG)	.3278	----
1b (e = .9)	.3314	-1.1%
2b (e = .96)	.4400	-34.23%
3b (e = .97)	.2800	14.6%
4b (32 nozzles)	.2670	18.55%
5b (75 nozzles)	.3091	5.7%
6b (32 nozz/out)	.2490	24.04%
7b (32 nozz/in)	.4340	-32.4%
8b (ACR = 9.045)	.2677	18.3%
9b (ACR = 23.06)	.2053	37.4%
10b (angle = 60)	.3232	0.5%
11b (angle = 75)	.3209	2.1%
12b (inj V = 160)	.3238	1.2%
13b (inj V = 250)	.3113	5.0%
14b ($\Delta X = 6.329$)	.3362	-2.5%
15b ($\Delta X = 4.329$)	.3652	-11.4%

APPENDIX C
Procedures for Changes to FASER Input

APPENDIX C

The purpose of this appendix is to describe how changes were made to the input for the meteorological and test configuration parametric study cases in this thesis. A detailed explanation of how to make changes and what changes can be made is available in Ref 6.

The procedures that must be followed to make changes to the meteorological parameters will be illustrated for the baseline condition. Procedures to vary the baseline condition follow similar logic.

The baseline condition required Mach = .55, altitude = 1000 feet, and total temperature = 480°R at the freejet exit. With these values and the physical dimensions of the test cell (Figure 3), it is then possible to calculate the remaining values needed for input. Working from the freejet exit upstream, first calculate the exit area

$$A = \pi r^2 \tag{1}$$

Assuming isentropic flow, the total pressure and static temperature can be calculated from the following relationships

$$T_T = T_S \left[1 + \left(\frac{\gamma - 1}{2}\right) M^2\right] \tag{2}$$

$$P_T = P_S \left[1 + \left(\frac{\gamma - 1}{2}\right) M^2\right]^{\frac{\gamma}{\gamma - 1}} \tag{3}$$

With static temperature calculated, the acoustic velocity is found from

$$a = \sqrt{\gamma RT} \tag{4}$$

The velocity of the gas flow then follows as

$$V = Ma \tag{5}$$

Assuming a perfect gas

$$\rho = \frac{P}{RT} \tag{6}$$

The mass flow through the ducting can be calculated using the mass flow parameter

$$MPF = \frac{\dot{m}\sqrt{(T_t)}}{P_T A} \tag{7}$$

where the MFP is tabulated as a function of Mach and specific heat ratio. The water flow rate per jet, WC, is equal to

$$WC = \frac{\dot{m}}{\rho} * LWC * \frac{1 m^3}{35.3 ft^3} * \frac{1 gallon}{3780 grams} * \frac{1 nozzle}{6 jets} * \frac{60 sec}{1 min} / \# nozzles \tag{8}$$

If evaporation is to be used, the LWC in the above calculation must be raised until the mean value of the LWC at the exit approximately equals the desired set value. This is an iterative process. Raising the LWC by 20% is a good first cut.

With the freejet exit parameters determined, and assuming no total property losses and steady flow conditions, the inlet conditions can be calculated. The duct area is determined as above. The Mach number is found by calculating the MFP from the equation above and searching through tables to find the corresponding Mach. With the Mach and the total properties, the static properties can be found from the equations above.

The bellmouth geometry must be obtained for the specific test cell desired. The J-1 configuration is shown in Figure 3. The number and location of sprays must be determined next. There are six sprays per nozzle, so for the

baseline condition there are 60 sprays. The (Y,Z) coordinate locations are with respect to the center of each nozzle. Since all nozzles are identical, the coordinates must simply be copied for the appropriate number of nozzles. The water flow rate per jet is input for WC. To set the mean droplet diameter, the droplet population must be broken down into discrete groups. DIAM indicates the droplet diameter in microns for a group of droplets. DPOP is the relative number density of droplets with diameter DIAM. The final input to the baseline condition is the coordinates of the nozzle center. The first y coordinate goes in OY and corresponds to the first z coordinate in OZ. The parameters changed from the baseline condition and their new values are listed in Table 2.

The test cell configuration parametric study required changes to geometric input in FASER. Several items were examined in the parametric study. They were the number of spray nozzles, the position of the spray nozzles, the eccentricity of the bellmouth, the area contraction ratio, the water injection velocity, the angle of the water injection and the distance between the spraybars and the bellmouth. The range of values and the reasons why they were chosen are given in chapter IV.

The coordinates of the spraybar nozzles must be known for a given test cell design to change the location or number. The user may choose any coordinates if a new spraybar system is to be designed. Figure 2 illustrates the spraybar system in test cell J-1. When changing the position of the spraybars, the new coordinates must be included in the input as OY and OZ. When changing the number of nozzles, the coordinates of the nozzles, the number of sprays, the coordinates of the jets and the water flow rate per jet must be changed following the procedures outlined in the meteorological

parametric study above. In performing the test cell configuration parametric study, it was desired to change the curvature of the bellmouth. The bellmouth curvature was thought to be responsible for heavier particles crossing their streamlines towards the center of the duct due to higher inertia. With more severe curvature, more particles would be forced to the center of the duct.

The curvature of bellmouths is typically defined by the shape of an ellipse (Ref 15). The eccentricity of the ellipse numerically describes the severity of the curvature. The eccentricity was used to compare between bellmouth geometric configurations.

The equations for an ellipse and eccentricity are listed below from reference 16:

$$\frac{(X-h)^2}{a^2} + \frac{(Y-k)^2}{b^2} = 1 \qquad (9)$$

$$e = \frac{\sqrt{a^2 - b^2}}{a} \qquad (10)$$

where (h,k) are the coordinates of the center of the ellipse with 2a and 2b being the major and minor axis, respectively. The bellmouth curve of the baseline configuration was examined to determine the values of a, b, and the ellipse center coordinates.

The center of the ellipse was seen from the baseline curvature to be at approximately h = 8.255, k = 2.926. With this information and the coordinates of the curve, the values of a and b were determined to be 2.926 and 1.093, respectively (Figure 31). From the values of a and b, the eccentricity was calculated to be .93 for the baseline configuration. For the

parametric study, it was decided to also examine bellmouths with eccentricities of .9, .96 and .97 in Cases 1b, 2b and 3b.

For Cases 1b and 2b, the value of b was maintained constant while varying the value of a to achieve the desired eccentricity. For Case 1b this turns out to yield a = 2.508 feet. Case 2b has a = 3.9 feet. The equation for an ellipse can then be algebraically manipulated as follows to obtain the coordinates necessary for use in the code.

$$Y = K - \left[\left(1 - \frac{(H-h)^2}{a^2}\right) b^2\right]^{1/2} \qquad (11)$$

These coordinates are only to be used for the curved portion of the bellmouth. At the bottom of the ellipse the Y values will be held constant while inputting different values of X to give the desired bellmouth length.

Once the bellmouth coordinates have been determined it is useful to plot the coordinates on graph paper. With a french curve a smooth contour may be drawn to connect the front lip of the bellmouth with the plenum entrance. The coordinates of this smooth curve must also be input with the bellmouth coordinates into the code. This smooth curve is then taken by the code to be a fixed boundary. The curve represents how the airflow will be forced to adjust in the test cell to meet the physical configuration of the plenum. This assumption is discussed in Chapter II. Figure 15 shows the new bellmouth curves of Cases 1b and 2b.

The area contraction ratio (area of the inlet/area of the exit) was varied by maintaining a constant inlet area and reducing the exit area. The freejet exit radius was reduced by one-half foot in Case 8b and then one foot in Case 9b. Several parameters need to be adjusted in the input. For this parametric study the eccentricity was maintained constant at .93. The

bellmouth y coordinates were reduced by one-half and one foot from the freejet exit to the lip of the bellmouth. New curves must then be drawn to join the bellmouth lip with the inlet. The plots of these curves are shown in figure 19. With a reduction in exit area, the mass flow through the test cell must be recalculated following equation 7 above. The Mach number is then calculated at the inlet using the same equation. The static pressure and temperature can be calculated using the isentropic relationships discussed previously.

The parameter VSMX is changed to vary the water injection velocity. PHIS is changed to vary the angle between the spray centerline and the gas flow. The final parameter to be varied was the distance between the spray nozzles and the bellmouth entrance. The bellmouth coordinates were changed to vary this distance.

NOMENCLATURE

A_i	Area of Individual Grid Element
Ad	Cross-Sectional Area of Droplet
A_T	Total Cross-Sectional Area
C_D	Droplet Drag Coefficient
C_μ	Turbulent Length Scale Coefficient
d	Droplet Diameter
g	Gravitational Acceleration
K	Turbulent Kinetic Energy
L_e	Turbulent Length Scale
LWC	Liquid Water Content
$\dot{m}$	Mass Flow of Gas Phase
M	Mach Number
m_d	Mass of Droplet
MDD	Mean Effective Droplet Diameter
P_s	Static Pressure
P_T	Total or Stagnation Pressure
R	Gas Constant
Re	Reynolds Number
t	Time
T_s	Static Temperature
T_T	Total or Stagnation Temperature
u, v	Axial and Radial Velocity Components of Gas Phase
X_i	I'th Value of X
X_m	Mean Value of any Parameter X

σ	Standard Deviation
Ψ	Stream Function
γ	Specific Heat Ratio
ρ	Density of Gas Phase
ρ_o	Stagnation Density
μ	Dynamic Viscosity
ε	Turbulent Dissipation

VITA

Jeffrey Ethan Haymond was born in Plattsburgh, New York on January 4, 1964. A military "brat," he moved often until finally residing in Rison, Arkansas. Following graduation from Rison High School, he accepted an appointment to the United States Air Force Academy. He graduated in May 1985 with a Bachelor of Science in Aeronautical Engineering.

The new 2nd Lieutenant Haymond was assigned to the Arnold Engineering Development Center, Arnold Air Force Station, Tennessee in July 1985. He enrolled at the University of Tennessee Space Institute in the Fall of 1985. He received the Master of Science with a major in Mechanical Engineering in August 1989.